NAVAL POSTGRADUATE SCHOOL

MONTEREY, CALIFORNIA

THESIS

SOURCE LOCALIZATION IN WIRELESS SENSOR NETWORKS WITH RANDOMLY DISTRIBUTED ELEMENTS UNDER MULTIPATH PROPAGATION CONDITIONS

by

Georgios Tsivgoulis

March 2009

Thesis Advisor:	Murali Tummala
Co-Advisor:	John McEachen
Second Reader:	T. Owens Walker III

Approved for public release; distribution is unlimited.

THIS PAGE INTENTIONALLY LEFT BLANK

REPORT DOCUMENTATION PAGE			Form Approved OMB No. 0704-0188
Public reporting burden for this collection of information is estimated to average 1 hour per response, including the time for reviewing instruction, searching existing data sources, gathering and maintaining the data needed, and completing and reviewing the collection of information. Send comments regarding this burden estimate or any other aspect of this collection of information, including suggestions for reducing this burden, to Washington Headquarters Services, Directorate for Information Operations and Reports, 1215 Jefferson Davis Highway, Suite 1204, Arlington, VA 22202-4302, and to the Office of Management and Budget, Paperwork Reduction Project (0704-0188) Washington DC 20503.			
1. AGENCY USE ONLY ***(Leave blank)***	**2. REPORT DATE** March 2009	**3. REPORT TYPE AND DATES COVERED** Engineer's Thesis	
4. TITLE Source Localization in Wireless Sensor Networks with Randomly Distributed Elements under Multipath Propagation Conditions.			**5. FUNDING NUMBERS**
6. AUTHOR(S) Georgios Tsivgoulis			
7. PERFORMING ORGANIZATION NAME(S) AND ADDRESS(ES) Naval Postgraduate School Monterey, CA 93943-5000			**8. PERFORMING ORGANIZATION REPORT NUMBER**
9. SPONSORING /MONITORING AGENCY NAME(S) AND ADDRESS(ES) N/A			**10. SPONSORING/MONITORING AGENCY REPORT NUMBER**
11. SUPPLEMENTARY NOTES The views expressed in this thesis are those of the author and do not reflect the official policy or position of the Department of Defense or the U.S. Government.			
12a. DISTRIBUTION / AVAILABILITY STATEMENT Approved for public release; distribution is unlimited.			**12b. DISTRIBUTION CODE**

13. ABSTRACT (maximum 200 words)

This thesis proposes a least-squares error estimator for line-of-sight, direction of arrival-based localization and a hybrid source localization scheme that addresses multipath propagation for non-cooperative sources using random arrays of wireless sensors. Taking advantage of the dominant reflections, the proposed solution finds the location of a signal source by triangulation using the direction of arrival estimations of both the line-of-sight and the reflected components. It uses a space division multiple access, spread spectrum-based receiver to generate the direction of arrival estimates. The time difference of arrival information is used to discriminate between the line-of-sight and the non-line-of-sight signals and to associate the incoming multipath signal with the corresponding source and reflector pair. In special cases, the proposed scheme is capable of solving the association problem spatially without the need for time difference of arrival information. Simulation results are included to demonstrate that the proposed scheme provides improved estimates by exploiting the non-line-of-sight information.

14. SUBJECT TERMS Wireless Sensor Network, Direction of Arrival, DOA, Random Arrays, Smart Antennas, Time Difference of Arrival, TDOA, Multipath Propagation, Source Localization			**15. NUMBER OF PAGES** 111
			16. PRICE CODE
17. SECURITY CLASSIFICATION OF REPORT Unclassified	**18. SECURITY CLASSIFICATION OF THIS PAGE** Unclassified	**19. SECURITY CLASSIFICATION OF ABSTRACT** Unclassified	**20. LIMITATION OF ABSTRACT** UU

THIS PAGE INTENTIONALLY LEFT BLANK

Approved for public release; distribution is unlimited.

SOURCE LOCALIZATION IN WIRELESS SENSOR NETWORKS WITH RANDOMLY DISTRIBUTED ELEMENTS UNDER MULTIPATH PROPAGATION CONDITIONS

Georgios Tsivgoulis
Lieutenant Junior Grade, Hellenic Navy
B.S., Hellenic Naval Academy, 2001

Submitted in partial fulfillment of the
requirements for the degrees of

ELECTRICAL ENGINEER

and

MASTER OF SCIENCE IN ELECTRICAL ENGINEERING

from the

NAVAL POSTGRADUATE SCHOOL
March 2009

Author: Georgios Tsivgoulis

Approved by: Murali Tummala
Thesis Advisor

John C. McEachen
Co-Advisor

T. Owens Walker III
Second Reader

Jeffrey B. Knorr
Chairman, Department of Electrical and Computer Engineering

THIS PAGE INTENTIONALLY LEFT BLANK

ABSTRACT

This thesis proposes a least-squares error estimator for line-of-sight, direction of arrival-based localization and a hybrid source localization scheme that addresses multipath propagation for non-cooperative sources using random arrays of wireless sensors. Taking advantage of the dominant reflections, the proposed solution finds the location of a signal source by triangulation using the direction of arrival estimations of both the line-of-sight and the reflected components. It uses a space division multiple access, spread spectrum-based receiver to generate the direction of arrival estimates. The time difference of arrival information is used to discriminate between the line-of-sight and the non-line-of-sight signals and to associate the incoming multipath signal with the corresponding source and reflector pair. In special cases, the proposed scheme is capable of solving the association problem spatially without the need for time difference of arrival information. Simulation results are included to demonstrate that the proposed scheme provides improved estimates by exploiting the non-line-of-sight information.

THIS PAGE INTENTIONALLY LEFT BLANK

TABLE OF CONTENTS

LIST OF FIGURES

LIST OF TABLES

THIS PAGE INTENTIONALLY LEFT BLANK

EXECUTIVE SUMMARY

A wireless sensor network (WSN) is an autonomous, self-organizing network without any pre-established infrastructure or centralized administration. WSNs have been used for a wide range of applications where, often, the main goal is to monitor a specified phenomenon. One important monitoring task which has recently caught the attention of WSN researchers is that of locating a signal source by extracting the information contained in the received signal. Two primary approaches to source localization have evolved: direction of arrival (DOA) based techniques and time difference of arrival (TDOA) based techniques

This thesis proposes a least squares error estimator for DOA localization which is unbiased when the noise is Gaussian-distributed with zero mean. This estimator solves an over determined Vandermonde system of equations which is known to be computationally efficient and accurate.

Based on this least squares error estimator, this thesis proposes a passive source localization scheme which exploits the non-line-of-sight (NLOS) signals from non-cooperative sources. The proposed solution is a hybrid DOA/TDOA source localization scheme and is comprised of three parts: a DOA estimator, an association algorithm for the identified signal bearings, and the source localization scheme itself. The recently proposed Space Division Multiple Access (SDMA)-based receiver is used for DOA estimation. TDOA information is used to discriminate between the line-of-sight (LOS) and the NLOS signals and to associate the incoming multipath signal with the corresponding source and reflector pair. In special cases, the proposed scheme is capable of solving the association problem spatially without the need for TDOA information. A technique is also provided to estimate the position and the orientation of the reflectors when site-specific database information is not available. Both centralized and distributed variants of the proposed scheme are presented with the latter being of particular interest in WSNs.

The proposed localization scheme allows a wireless sensor network to (1) perform single array localization, (2) perform the localization in a distributed fashion, (3) obtain source location estimates with NLOS signals only and (4) improve the location estimates compared with those obtained using the LOS information only.

A simulation model was developed and implemented in MATLAB to evaluate the performance of the proposed localization scheme. The simulation results demonstrate that the proposed localization scheme provides high accuracy estimates and outperforms the LOS-only based localization schemes. This is primarily because more bearings are available and the conditioning of the least squares problem is better for the proposed scheme. Furthermore, the simulation results also show that the proposed scheme is able to provide accurate NLOS-only source location estimates when the LOS paths are not available.

ACKNOWLEDGMENTS

I would like to express my outmost appreciation to Professor Murali Tummala for his valuable advice throughout this thesis. He made this process an engaging learning experience for me.

I would like to thank Professor John McEachen for his time and effort in reviewing this thesis and valuable feedback contributed.

My gratitude to CDR Owens Walker III for his valuable help during this thesis and for the countless hours spent with me to make this thesis a technical document and to teach me how to write.

I would also like to thank my parents John and Maria for giving me an insatiable desire to learn.

Most importantly I would like to express my heartfelt gratitude to my beloved wife, Christina, for her endless patience and support, as well as my little daughter, Mara, who inspired me and gave me many beautiful moments while I was working with this thesis.

THIS PAGE INTENTIONALLY LEFT BLANK

I. INTRODUCTION

A. INTRODUCTION TO PASSIVE SOURCE LOCALIZATION USING WIRELESS SENSOR NETWORKS

A wireless sensor network (WSN) is an autonomous, self-organizing network without any pre-established infrastructure or centralized administration [1]. WSNs have been used for a wide range of applications where, often, the main goal is to monitor a specified phenomenon [2]. Wireless sensor networks offer numerous advantages when compared to traditional wired or wireless networks [3]. Of particular interest, WSNs provide greater redundancy since the malfunction of a number of sensors has less impact on the overall system performance. Additionally, WSNs can be deployed quickly at low cost and are well-suited to use in mobile platforms. Not surprisingly, they have found wide-spread interest in emergency and military applications.

One important monitoring task which has recently caught the attention of WSN researchers is that of locating a signal source by extracting the information contained in the received signal. That source could be an enemy's radio location, as in military applications, or the direction of arrival (DOA) and the location of a sensed phenomenon in an emergency situation like the seismic waves which follow an earthquake [3]. A WSN performs the source localization by coordinating the effort of individual sensors which act as antenna elements. These sensors are clustered together to form antenna arrays which fuse the data collected by the sensors, to carry out the localization task [4].

B. RELATED WORK IN PASSIVE SOURCE LOCALIZATION WITH WIRELESS SENSORS NETWORKS

Passive source localization using wireless sensor arrays is a problem addressed extensively in existing literature. Two primary approaches to source localization have evolved [5]: direction of arrival (DOA) based techniques and time difference of arrival (TDOA) based techniques. DOA-based localization systems utilize antenna arrays which examine the spatial characteristics of the incident signals to obtain bearing estimates [11], [12], [13], [14], [15] and [16]. The bearing estimates are used for the position location determination by triangulation [5] [17], [18] and [19]. TDOA localization systems

estimate the source location using the intersection of hyperboloids, which are the set of range difference measurements between three or more receiving sensors. These are determined by measurement of the TDOA of a signal between the sensors [2], [6], [7], [8], [9], and [10].

The need for accurate localization requires knowledge of the spatial characteristics of the wireless channel since those characteristics significantly affect the performance of the arrays. Thus, a significant challenge is the development of realistic channel models which can accurately predict the behavior of the wireless medium [30]. In a real-world deployment, complex propagation phenomena lead to uncertainty in deciding whether a direction of arrival (DOA) corresponds to the line-of-sight (LOS) signal or its reflection [2]. That uncertainty can lead to significant errors when estimating the position of the desired source. The problem is more severe when a LOS signal does not exist as is often the case in urban environments. Additionally, it has been reported that a number of strong reflections can be expected even in rural areas [31]. These non-line-of-sight (NLOS) signals potentially provide additional information that can be exploited in the source location.

There have been several proposals in literature that consider the presence of NLOS signals. The first category is comprised of schemes which attempt to mitigate the effects of the NLOS signals. In [22], the measurements are weighted to emphasize the LOS signals, while [23] identifies the arrays that do not receive LOS signals and excludes them from the localization process. In both approaches, the authors seek to minimize the impact of the NLOS signals rather than taking advantage of them. Recently, a second category of solutions is beginning to emerge that attempts to exploit these NLOS signals. The authors of [24] propose a hybrid DOA/TDOA scheme which exploits the NLOS when the desired source is cooperative.

In contrast, this thesis proposes a passive source localization scheme which exploits the NLOS signals from non-cooperative sources. It is a DOA/TDOA-based scheme which uses bearing estimation for localization through triangulation. The TDOA information is used to discriminate between the LOS and the NLOS signals and to

associate the incoming multipath signal with the corresponding source and reflector pair. Furthermore, using the NLOS information, the proposed scheme is capable of performing single array localization.

C. THESIS OBJECTIVE

The objective of this research is to develop a source localization scheme that is capable of non-cooperative source localization within the constraints of a WSN. The existing work on cooperative source localization can then be viewed as a special case of this more general solution.

There are two significant contributions in this work. The first is a proposed least squares estimator for DOA-based localization. The second is a passive source localization scheme which exploits the NLOS signals from non-cooperative sources. The latter is a DOA/TDOA-based scheme which uses bearing estimation for localization through triangulation. The TDOA information is used to discriminate between the LOS and the NLOS signals and to associate the incoming multipath signal with the corresponding source and reflector pair. Furthermore, using the NLOS information, the proposed scheme is capable of performing single array localization or NLOS only based localization. Both centralized and distributed variants of the proposed scheme are presented with the latter being of particular interest in WSNs.

D. THESIS OUTLINE

Chapter II provides the background to support the proposed work. It introduces the fundamental concepts of antenna arrays including the response of an array with randomly distributed elements. An overview of the wireless environment is also included to validate the adopted propagation and received signal models. The chapter then outlines several current approaches to DOA estimation. The recently proposed Space Division Multiple Access (SDMA)-based receiver is presented and compared to the conventional MUSIC algorithm. Chapter II closes with a brief discussion of TDOA estimation.

The significant contributions of this work are presented in Chapter III. Examining LOS-only localization first, a least-squares estimator for DOA localization is proposed and analysis is provided to investigate the biasing, the impact of errors, and the

conditioning of the proposed estimator. A comparison between the least-squares and the total-least-squares solutions is also presented. To take advantage of a long duration signal, a sequential least-squares approach is also included. Turning our attention to NLOS as well as LOS signals, the proposed localization scheme which exploits the NLOS signals is then described. The incident signal-source-reflector association algorithm is outlined and a technique is provided to estimate the position and the orientation of the reflector. Chapter III concludes with the source localization procedure of the proposed scheme.

In Chapter IV, simulation results are provided to evaluate the performance of the proposed scheme and compare it to existing LOS-only solutions.

Chapter V summarizes the significant contributions of this thesis and provides some ideas for extending this work in the future.

Finally, the Appendix includes the MATLAB code used in the simulation.

II. BACKGROUND ON SOURCE LOCALIZATION

This chapter provides the background to support the proposed solution for passive source localization of non-cooperative sources using clusters of random or aperiodic sensor arrays which form a wireless sensor network (WSN). In this thesis, we consider a hierarchical WSN that consists of two levels. The top level is the network of arrays in which each array is viewed as a single node. These nodes perform the DOA estimation task and the bearings obtained are transmitted to a fusion center, where the localization algorithm is executed. In the proposed distributed variant of our solution, each node also performs single-array localization. In this case, the source location estimations are then simply averaged by the data fusion center. In the second level of the WSN, each array contains a number of sensor elements. DOA estimation is conducted at this sensor layer, while the source localization is conducted at the array level. An example WSN is shown in Figure 1.

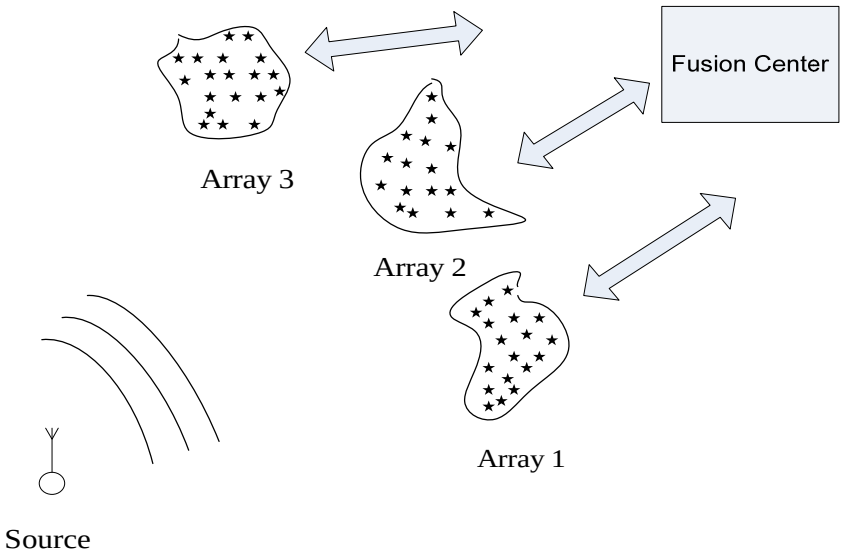

Figure 1. Example WSN comprised of 3 arrays, a single source of interest and a fusion center.

This chapter begins by discussing the array response to an incident signal. An overview of the propagation environment follows and a propagation prediction model is adopted to provide a realistic scenario for performance comparison of the localization schemes. A link budget analysis is then conducted and the signal received by the array is computed. Finally, this chapter closes with a discussion of both DOA estimation and TDOA estimation. Two methods of DOA estimation are presented, the Multiple Signal Classification (MUSIC) DOA estimation method [26] and the new Space Division Multiple Access (SDMA) receiver [25]. A comparison of the angle resolution and the accuracy of both algorithms is included and the SDMA receiver is chosen as the DOA estimation method of the localization process in this thesis. The TDOA estimates will be used to associate the multipath components of the received signal with the corresponding source and the related reflectors.

A. ARRAY RESPONSE

The array steering vector contains the responses of all sensors to a source with a single frequency of unit power [26]. The array response varies as a function of direction and a steering vector is associated with each direction of interest. The uniqueness of the association is defined by the array configuration [27]. In this section, we begin with a discussion of linear arrays followed by the more general case of two-dimensional aperiodic and random arrays.

1. Uniform Linear Array (ULA)

The configuration of a uniform linear array (ULA) is shown in Figure 2. The source transmits a narrow band signal $s(t)$ of frequency f and is assumed to be in the far field. The array consists of N sensors with uniform inter-element spacing d. With respect to the reference node (sensor 1), sensor 2 experiences a time delay of [28]

$$\Delta\tau = \frac{d\cos\theta}{c} \tag{1}$$

where c is the signal propagation speed. The time delay $\Delta\tau$ corresponds to a phase shift of the signal equal to

$$\Delta\psi = 2\pi \frac{d\cos\theta}{\lambda}. \tag{2}$$

This phase shift is the same for every pair of sensors because the inter-element spacing is constant (uniform). Assuming identical sensor elements, the steering vector of this array is given by

$$\bar{a}(\theta) = \begin{bmatrix} 1 & e^{-j\Delta\psi} & \ldots & e^{-j(N-1)\Delta\psi} \end{bmatrix} \tag{3}$$

which can in turn be written as

$$\bar{a}(\theta) = \begin{bmatrix} 1 & e^{-j\frac{2\pi}{\lambda}d\cos\theta} & \ldots & e^{-j(N-1)\frac{2\pi}{\lambda}d\cos\theta} \end{bmatrix}^{\mathrm{T}}. \tag{4}$$

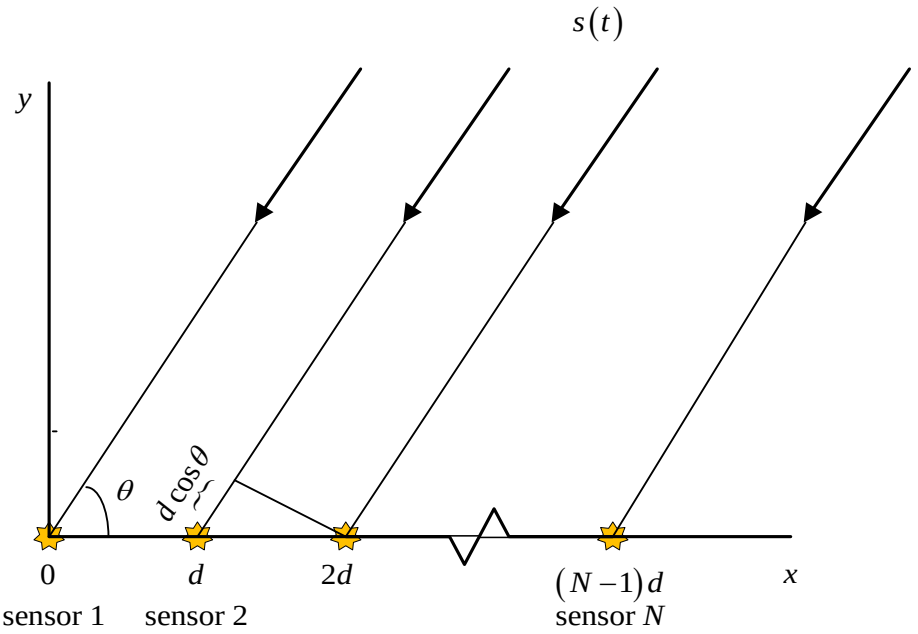

Figure 2. Uniform linear array of N sensors with inter-element spacing d. The source is located in the far field.

2. Two-Dimensional Aperiodic and Random Arrays

The geometry of a two-dimensional aperiodic array is shown in Figure 3. The sensors of the array are placed in the x-y plane according to some algorithm. Without a

loss of generality, the position of the reference sensor is assumed to be at the origin of the coordinate system. The phase difference between sensor i and the reference sensor is given as

$$\Delta\psi = \frac{2\pi}{\lambda}\left(x_i \cos\theta + y_i \sin\theta\right) \tag{5}$$

and thus the corresponding steering vector is found to be

$$\bar{a}\left(\theta\right) = \begin{bmatrix} 1 & e^{-j\frac{2\pi}{\lambda}\left(x_2\cos\theta + y_2\sin\theta\right)} & \cdots & e^{-j\frac{2\pi}{\lambda}\left(x_i\cos\theta + y_i\sin\theta\right)} \end{bmatrix} \tag{6}$$

When the positions of the sensors are chosen by some random process, the aperiodic array is known as random array [29]. The steering vector of the random array is identical to that of the aperiodic array except that the vector $\left(\tilde{x}_i, \tilde{y}_i\right)$ is a random vector as in

$$\bar{a}\left(\theta\right) = \begin{bmatrix} 1 & e^{-j\frac{2\pi}{\lambda}\left(\tilde{x}_2\cos\theta + \tilde{y}_2\sin\theta\right)} & \cdots & e^{-j\frac{2\pi}{\lambda}\left(\tilde{x}_i\cos\theta + \tilde{y}_i\sin\theta\right)} \end{bmatrix} \tag{7}$$

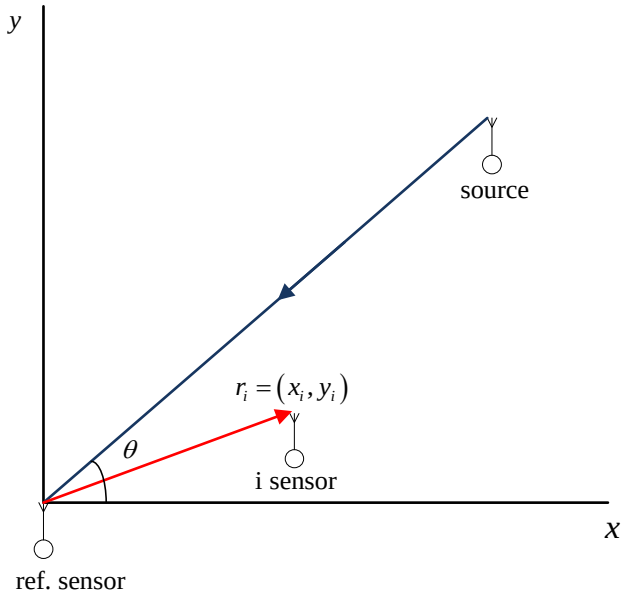

Figure 3. Two-dimensional array geometry.

This thesis considers aperiodic, random arrays. Aperiodic sensor arrays have several advantages when compared to conventional periodic sensor arrays. Due to the non-periodic nature of the sensor spacing, they do not suffer from grating lobes in their

spectrum and are not limited to a maximum sensor separation of 0.5 λ (0.5 m at 300 MHz) [29]. This reduces the cost of the construction of such an array, since a smaller number of sensors are required. Larger element separation also provides more resilience against mutual coupling [29] which occurs between the sensors when one is in the vicinity of the other [26]. This coupling effect degrades array performance and is largely ignored in most array signal processing literature. Finally, random arrays provide flexibility in deployment and can accommodate arbitrary topologies, which are common in mobile platforms and WSNs.

B. SOURCE TO ARRAY

In this section, we discuss and adopt a radio propagation model of the wireless communications channel that will be used in the subsequent performance. Free space path loss causes signal strength attenuation of a LOS electromagnetic wave, while with NLOS, multipath components can also be attenuated due to reflection, diffraction, and scattering [31]. Electromagnetic signals experience attenuation while they travel in space. This is the result of spherical energy spread in space. Reflection occurs when a signal strikes a surface and is then reflected towards the receiver. Diffraction is the phenomenon that occurs when the electromagnetic signal strikes the edge of the corner of a large structure compared with the wavelength. Scattering occurs when a signal strikes an object that is much smaller compared with the wavelength [32]. These effects lead to complex multipath propagation scenarios, especially in areas with a high density of potential reflectors and scatterers (e.g., in urban areas).

1. Propagation Environment

In this section, we look at signal attenuation in both line-of-sight and reflected signals. We present loss expressions for both.

a. Free Space Loss

In wireless communications, as the signal propagates through the medium, it disperses with distance [33]. This type of attenuation, known as free space loss (L_s), can be expressed as the ratio of the signal power between the transmitter and the receiver in dB as

$$L_s = 10\log\frac{P_t}{P_r} = 20\log\left(\frac{4\pi d}{\lambda}\right) = -20\log(\lambda) + 20\log(d) + 21.98 \text{ dB} \qquad (8)$$

where P_t is the transmitted signal power, P_r is the received signal power, and d is the distance between transmitter and receiver. The free space loss is proportional to the square of the distance between the transmitter and the receiver. Thus, as this distance is increased, the free space attenuation becomes very large.

b. Reflection

When a signal propagating in one medium encounters the boundary of another medium, it is partially reflected back to the first medium and partially refracted to the new medium [21]. The propagation characteristics of the resulting waves are governed by the boundary conditions of the interface.

A schematic representation of the reflection on a smooth surface is shown in Figure 4. The relationships for the angles shown in the figure are given by Snell's law as

$$\begin{aligned} &\theta_I = \theta_R \quad \text{and} \\ &\sin\theta_R = \sqrt{\varepsilon_r}\sin\theta_T \end{aligned} \qquad (9)$$

where ε_r is the dielectric constant of the material. The attenuation of the reflected signal is given by the square of the reflection coefficient as in $P_R = P_I|\Gamma|^2$. The reflection coefficient, Γ, is a function of the reflected and refracted angles and has a range between 0 and 1. This coefficient depends on the type of polarization. Thus, for transverse-electric (TE) polarized plane, it can be shown to be [21]

$$\Gamma_{\mathrm{E}} = \frac{\cos\theta_R - \sqrt{\varepsilon_r}\cos\theta_T}{\cos\theta_R + \sqrt{\varepsilon_r}\cos\theta_T}\ , \qquad (10)$$

while for transverse- magnetic (TM) polarized plane it is [21]

$$\Gamma_H = \frac{\sqrt{\varepsilon_r}\cos\theta_R - \cos\theta_T}{\sqrt{\varepsilon_r}\cos\theta_R + \cos\theta_T}. \qquad (11)$$

For $\varepsilon_r = 5$, Figure 5. plots the absolute value of the reflection coefficient for both types of polarization as a function of the incident angle. For TM polarization, there exists a single incident angle at which $\Gamma_{\mathrm{H}} = 0$ and no reflection occurs. This angle is called the Brewster angle and is expressed as [31]

$$\sin\left(\theta_{\mathrm{B}}\right) = \frac{\sqrt{\varepsilon_r - 1}}{\sqrt{\varepsilon^2{}_r - 1}} \quad . \tag{12}$$

On the other hand, when the incident angle is 90°, $\left|\Gamma_E\right| = \left|\Gamma_H\right| = 1$ and the signal is totally reflected for both types of polarization. The path loss because of the refection is

$$L_R = -20\log\left(\left|\Gamma\right|\right) \tag{13}$$

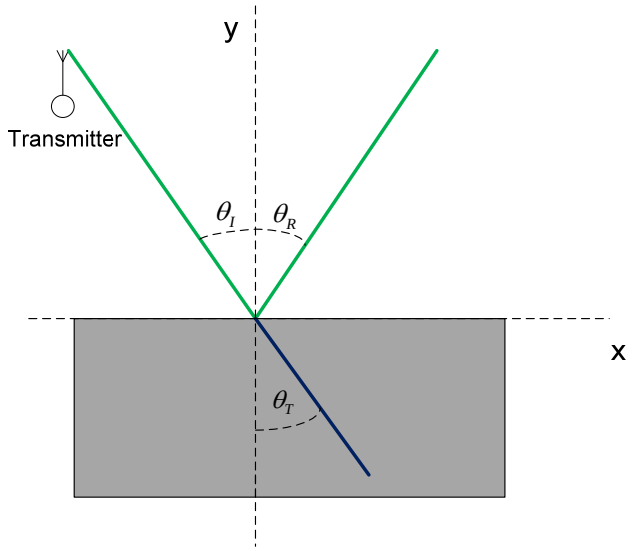

Figure 4. Geometrical representation of the reflection. The incident signal with angle θ_{I} is partially reflected with angle θ_R and partially refracted with angle θ_T

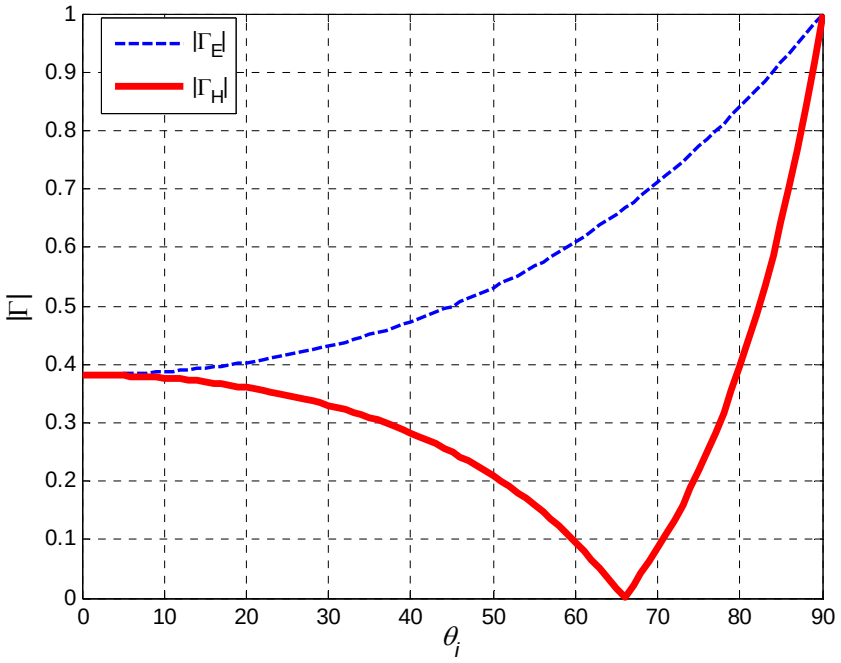

Figure 5. $|\Gamma|$ as a function of the incident angle for $\varepsilon_r = 5$.

2. Radio Propagation Prediction

Shifting our attention to the multipath effects, the classic radio propagation models provide information about the signal power and Doppler shifts of the received signal [30]. However, in source localization schemes, the time delay spread and the angle-of-arrival spread are also of major importance. A fundamental challenge in localization applications is therefore the development of realistic channel models that can accurately predict the characteristics of the multipath propagation. These propagation models are highly dependent upon the propagation environment and there does not exist a single model that covers every environment. Rather, several empirical models have been proposed based on measurements from different areas within the specific environment of interest. In general, the characterization of these environments is based upon the population density and the building architecture (e.g., urban, suburban, and rural). The most challenging propagation environment, particularly for source localization problems, is the urban environment where the received signal may be dominated by strong

reflections and the LOS path is not always present. A typical propagation scenario can be seen in Figure 6 and this thesis primarily focuses on this source localization problem in urban environments.

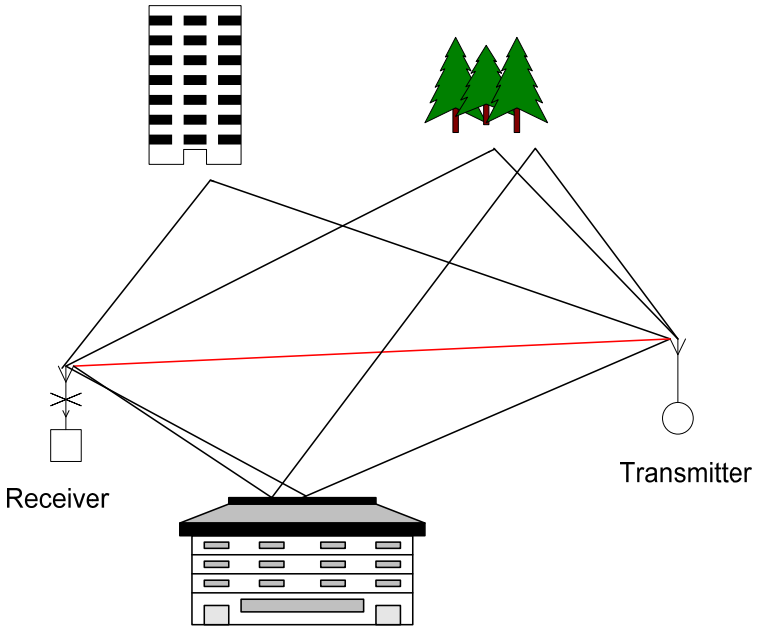

Figure 6. Typical propagation scenario. A LOS path and several NLOS paths are shown.

a. Site-Specific Propagation Prediction

Most propagation prediction models for urban areas examine the statistical parameters of the propagation environment, such as average row spacing and building height distributions [21]. That methodology is suitable when the aim of the model is the prediction of the average power of the signal received. However, applicability is limited in localization applications where the localization scheme is actively attempting to exploit the NLOS components of the signal.

As an alternative, the site-specific prediction model takes advantage of the actual mapping of the area under consideration. The mapping can be exploited by using a database which contains the footprints of the buildings and any other large objects [21]. Those databases must be, in general, three-dimensional. In the special case when the assumption of low antennas in tall building environments holds, the databases can be

two-dimensional. This is because, in those cases, the primary propagation paths lie around the sides of the buildings and no significant propagation paths exist over the rooftops [21].

Site-specific propagation models use ray optical methods and treat each reflection as an individual ray in the space. The maximum number of reflections along a ray path could be anywhere from six to eight and the number of walls in the database on the order of thousands [21] — facts which make the prediction a complex procedure. Additionally though (theoretically) the total received power is given by the summation of the powers of the individual rays; this strategy does not give a very accurate estimate because it ignores the scattered signals. Finally, the accuracy of the databases is on the order of 0.5 m in the best case [21], which introduces further uncertainty into the prediction.

All of this notwithstanding, a site-specific approach offers a simplifying feature when applied to source localization. When a ray path includes many reflections, the power delivered by the ray is reduced dramatically due to the attenuation of each reflection and the increased path length. In many cases, only the first reflections are strong enough to be exploited. Thus, the power of each individual ray is more important in the DOA estimation problem than the total received power and ignoring the contribution of the weak components can be an advantage. The localization procedure is significantly simplified by ignoring the multi-reflected rays, which could not be exploited anyway.

With respect to the size of the reflector, there is a limitation on the size of the region over which reflections occur and ray methods can be used. This can be understood by looking at Figure 7 in which a ray from the source is reflected by the reflector as shown. The length of the reflector surface is w_B, while $2w_F$ is the width of the Fresnel zone, defined by the relative geometry between the receiver and the reflector. If $w_B \cos\theta \geq 2w_F$, then the rules for reflection can be used in order to predict the propagation characteristics [21]. However, since $\max\{2w_F\} = \sqrt{\lambda S}$ where S is the total length of the reflected ray in meters, the maximum ray length is then bounded by

$$S \le \frac{1}{\lambda}\left(w_B \cos\theta\right)^2 . \tag{14}$$

Thus, if $\theta = 45^o$, $w_B = 20$ m, and $\lambda = 0.5$ m, (14) limits the ray length to 400 m. If the above inequality does not hold, then the object acts as a scatterer [34].

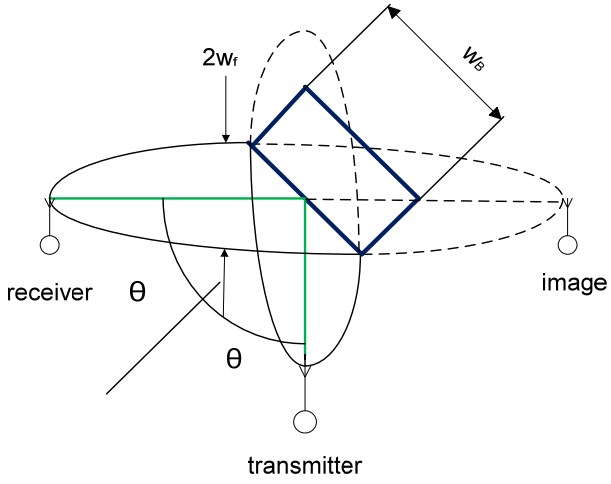

Figure 7. Fresnel zone and reflector surface characteristics [From 21].

b. Scattering Prediction

The propagation rays, as discussed in the previous section, were considered discrete lines in space which possess the total power of the corresponding multipath component. However, in reality, the power of the signal is distributed around these rays which deteriorate the accuracy of the DOA estimation methods. The distribution of the power around the ray is the result of the signal scattering caused by small objects found around the source. The same phenomenon is observed around the reflections which can be considered secondary sources. Thus, the scatterers are grouped into clusters, around both the source and the reflectors.

Several models have been proposed in literature to predict this scattering. The distribution of the angles of arrival caused by the scattering can be modeled as discrete Gaussian [30] or discrete Laplacian [35] as in

$$P_G(\theta) = c_1 e^{-\frac{\theta^2}{2\sigma^2}} \quad \text{Gaussian}$$
$$P_L(\theta) = c_2 e^{-\frac{\sqrt{2}|\theta|}{\sigma}} \quad \text{Laplacian} \tag{15}$$

where $\theta \in [-\pi, +\pi]$ and the mean value of both functions is the angle which corresponds to the associated ray. The parameter σ controls the spread of the functions. Typically, σ is small and the values of both functions are concentrated around the mean. A plot of the function for σ = 3 is shown in Figure 8. Measurements in [36] indicate that the distribution of the incident angle fits the discrete Laplacian function better, since in both rural and urban environments, they tend to demonstrate a sharp peak while also maintaining long tails.

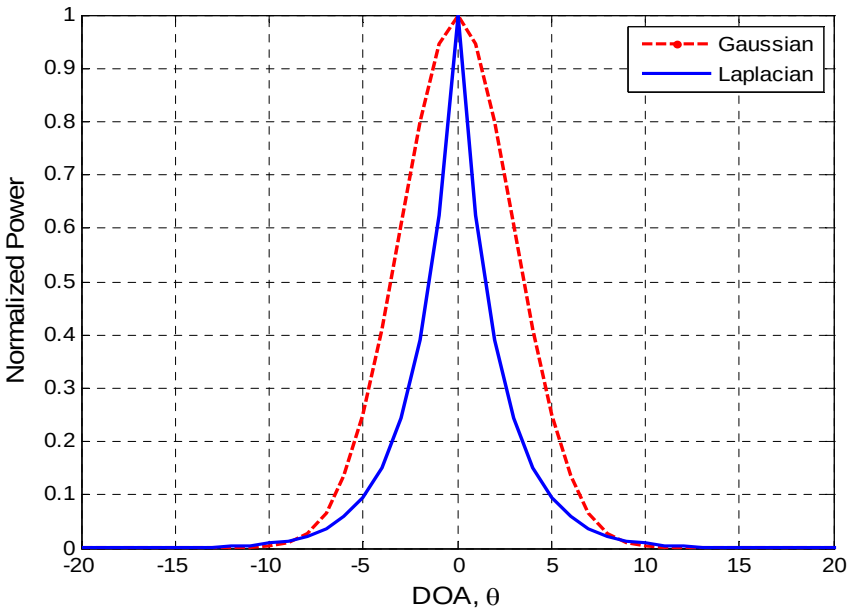

Figure 8. Gaussian versus Laplacian scattering functions.

3. The Adopted Propagation Model

In summary, the propagation model used in this thesis combines elements from the majority of the models discussed above. In a site-specific propagation model, the power attenuation of each ray is calculated as the sum of the path loss and the reflection attenuation. The site-specific mapping provides the number of reflectors encountered by

the ray en route to its destination and the path loss is computed using the free space path loss model for each ray individually. The total power of the received signal is the summation of the powers of the individual rays.

C. RECEIVED SIGNAL

The received signal model assumes multiple, uncorrelated sources transmitting signals to an N-sensor array. In this section, a link budget analysis is performed and the received signal-to-noise ratio (SNR) of the incoming signals is computed. Additionally, a matrix expression is defined for the received signal as a function of the response of the receiving array.

1. Link Budget Analysis

The power level of the incident signals is computed by subtracting the losses due to attenuation, as described previously, from the transmitted power and by adding the gain of the array. The gain of the array is given in dB as [29]

$$G_{AR} = 10\log\left(N\right) + G_{EL} \tag{16}$$

where G_{EL} is the gain of each array element in dB. Expression (16) holds for both ULA and aperiodic arrays, although in the latter case, it must be considered an approximation [37]. The link budget equation in dB for each signal path is then expressed as

$$SNR_{AR} = SNR_{SC} - L_S - L_R + G_{AR} + G_T \tag{17}$$

where SNR_{AR} is the signal-to-noise ratio available at the receiving array for a specific signal path, SNR_{SC} is the signal-to-noise ratio of the signal transmitted from the corresponding source L_s is the free space loss, L_R is the path loss because of the reflection, G_T is the transmitter gain (assumed to be 0 dB in this work) and G_{AR} is the array gain. The SNR for signal power P is defined in dB as

$$\text{SNR} = 10\log\left(\frac{P}{kTB}\right) \tag{18}$$

where k is the Boltzmann constant equal to 1.38×10^{-23} m^2 kg s^{-2} K^{-1}, T is the system noise temperature in degrees Kelvin which includes both the antenna and receiver noise and B is the effective noise bandwidth of the receiver.

2. Received Signal Model

Although the signal of each source is considered narrowband in the previous discussion, the results can be extended to wideband signals, given the assumption that the frequency response of the array is flat over the signal's bandwidth and the propagation time across the array is small when compared to the inverse of the bandwidth [26]. If the number of sources is *K* and each of them transmits a signal $s_k(t)$, the received signal at time t in the array can be expressed as

$$\bar{x}(t) = \sum_{k=1}^{K} \bar{a}(\theta_k) s_k(t) + \bar{n}(t) \tag{19}$$

where

$$\bar{x}(t) = \begin{bmatrix} x_1(t) & x_2(t) & \ldots & x_N(t) \end{bmatrix}^T \in \mathbb{C}^N, \tag{20}$$

$\bar{n}(t)$ is the noise vector and $\bar{a}(\theta_k)$ is the steering vector for signal $s_k(t)$ with DOA θ_k. In matrix notation, (20) can be written as

$$\bar{x}(t) = A(\bar{\theta})\bar{s}(t) + \bar{n}(t) \tag{21}$$

where $A(\bar{\theta}) \in \mathbb{C}^{N\times K}$ is the array response matrix which contains the responses of each sensor for each incident signal and is given as

$$A(\bar{\theta}) = \begin{bmatrix} \bar{a}(\theta_1) & \bar{a}(\theta_2) & \ldots & \bar{a}(\theta_k) \end{bmatrix} \tag{22}$$

and $\bar{\theta}$ is a vector which contains the DOA for each incoming signal. Let L be the number of observations with $L > K$. The received signal can then be written as

$$X = A(\Theta)S + N\,, \tag{23}$$

where $N \in \mathbb{C}^{N\times L}$ is the noise matrix and S $\in \mathbb{C}^{K\times L}$ is the transmitted signal matrix .

D. DOA ESTIMATION

This section discusses and compares two methods of DOA estimation, the Multiple Signal Classification (MUSIC) estimation and the Space Division Multiple Access (SDMA) receiver.

1. The MUSIC Algorithm

Most DOA algorithms are based on the computation of the signal correlation matrix [32]. The received signal correlation matrix R_{xx} and the desired signal correlation matrix R_{ss} are defined as

$$R_{xx} = E\left\{x(t)\,x^H(t)\right\} \tag{24}$$

$$R_{ss} = E\left\{s(t)\,s^H(t)\right\} \tag{25}$$

where H denotes the Hermitian transpose of the matrix and $E\{a\}$ is the expectation of the argument a [26]. If the statistics of the signal and the noise are not known but the corresponding processes are ergodic, then the correlation matrices can be approximated by averaging a finite number of data observations as [26]

$$\hat{R}_{xx} = \frac{1}{L}\sum_{l=1}^{L} \overline{x}(t_l)\overline{x}^H(t_l) \tag{26}$$

$$\hat{R}_{ss} = \frac{1}{L}\sum_{l=1}^{L} \overline{s}(t_l)\overline{s}^H(t_l)\,. \tag{27}$$

Both $\hat{R}_{ss}$ and $\hat{R}_{xx}$ are $N\times N$ matrices. If additive white Gaussian noise is assumed, the two matrices are related as [26]

$$\hat{R}_{xx} = A(\Theta)\hat{R}_{ss}A^H(\Theta) + \sigma^2{}_n I \tag{28}$$

where $\sigma^2{}_n$ is the noise variance and I is an $N\times N$ identity matrix. If the incident signals are uncorrelated, $\overline{R}_{ss}$ is diagonal. When the signals are coherent, $\overline{R}_{ss}$ is singular [38]. In

most cases, the signals are partially correlated and $\bar{R}_{ss}$ is positive definite. This property is very important, since, as will be shown later, the DOA estimation algorithms are based on the inversion of $\hat{R}_{ss}$. $\hat{R}_{xx}$ has N eigenvalues $(\lambda_1, \lambda_2, \ ... \ , \lambda_N)$ and N associated eigenvectors $\hat{E} = [\hat{e}_1 \quad \hat{e}_2 \quad ... \quad \hat{e}_N]$ which can be obtained by the eigenvalue decomposition. By ordering the eigenvalues from larger to smaller, the eigenvector matrix can be divided into two sub-matrices [32]

$$\hat{E} = \left[\hat{E}_s \quad \hat{E}_n \right]. \tag{29}$$

These sub-matrices are also called subspaces. $\hat{E}_s$ has K columns and corresponds to the signal subspace, while $\hat{E}_n$ has $N - K$ columns and corresponds to the noise subspace. An alternate way to find the eigenvectors of the autocorrelation matrix is directly to use the received signal matrix X and eigendecompose it by using the singular value decomposition (SVD), which gives more stable algorithms [39].

The Multiple Signal Classification (MUSIC) [26] is the most popular among the DOA algorithms based in the subspace decomposition of the correlation matrix. The desired DOAs are estimated by identifying the peaks of the MUSIC spatial pseudospectrum, which is given as [40]

$$P_{MUSIC} = \frac{a^H(\theta) a(\theta)}{a^H(\theta) E_n E^H{}_n a(\theta)}. \tag{30}$$

The array steering vectors are orthogonal to the noise subspace and, therefore, the peaks in the pseudospectrum represent the DOAs for the desired signal.

MUSIC can be applied to any arbitrary but known array topology [26] and accordingly, requires accurate array calibration [17]. Furthermore, MUSIC assumes the number of sources is known in order to assign the corresponding eigenvectors to the signal subspace and several algorithms have been proposed to do this [41]. Additionally, conventional MUSIC breaks down under near-coherent signal conditions like those which exist when multipath propagation conditions are present [32]. Again, several methods have been proposed to address this, but they are either applicable only to special

cases such as spatial smoothing which works for ULA [17] or they are computationally intensive such as multidimensional MUSIC [17].

2. The SDMA Receiver

The SDMA receiver is a new method for DOA estimation proposed in [25]. A depiction of this receiver is shown in Figure 9. The SDMA receiver does not rely on the subspace decomposition of the correlation matrix, rather it cross-correlates the received signal with a pre-computed set of array responses for every direction of interest.

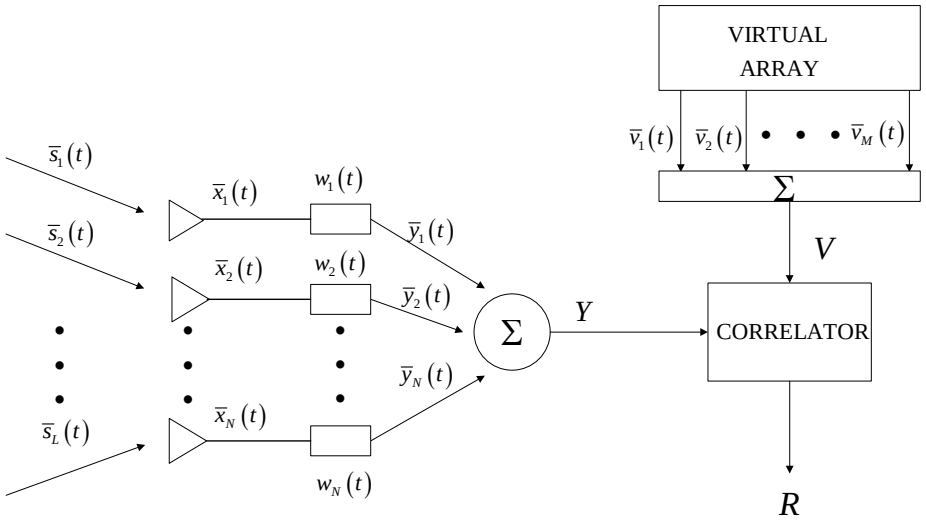

Figure 9. SDMA receiver [From 32].

From Figure 9, consider an N sensor array. The output of each array element $\bar{x}_n(t)$ is phase-modulated by a set of uncorrelated spreading sequences $\bar{w}_n(t)$. These sequences can be any type of pseudorandom [32] or orthogonal [37] sequence. The produced array outputs are then orthogonal or nearly orthogonal. In matrix notation, the output of the array is found to be

$$Y = W^H X \tag{31}$$

where X is given from (22) and $W \in \mathbb{C}^{N \times L}$ is the matrix of the spreading sequences which is defined as

$$W = \left[\bar{w}_1(t) \quad \bar{w}_2(t) \quad \ldots \quad \bar{w}_N(t) \right]^H. \tag{32}$$

The signals stored in the virtual array are also modulated by the same set of spreading sequences. In matrix notation, the output of the virtual array is given as

$$V = W^H A_M(\Theta), \tag{33}$$

where $A_M(\Theta) \in \mathbb{C}^{N \times L}$ is the matrix of the array responses of all sensors for all DOAs. The correlator cross-correlates the array signal with that of the output of the virtual array as in

$$R = V^H Y \tag{34}$$

where R is a $K \times L$ matrix. The spatial spectrum of the SDMA receiver is then

$$P_{SDMA} = |R_k| \tag{35}$$

where

$$R_k = \left[\sum_{l=1}^{L} R(1,l) \quad \sum_{l=1}^{L} R(2,l) \quad \ldots \quad \sum_{l=1}^{L} R(K,l) \right]. \tag{36}$$

The peaks of P_{SDMA} correspond to the DOAs of the incident signals.

The array used by the SDMA receiver is preferably a two-dimensional random array such that the sensor geometry and element phasing is unique for each DOA [32]. The spreading technique used further ensures that all received directions of interest are uniquely defined. The receiver does not compute the correlation matrix, but just correlates the received signal with a pre-computed one. Thus, in contrast to MUSIC, it does not rely on the correlation matrix properties. Also, the SDMA receiver does not require knowledge of the number of incident signals. Finally, the SDMA receiver does not rely on any complex adaptive or slow iterative methods. It “looks” in pre-determined, finite set of directions of interest [32] which, by estimating multiple angles simultaneously, translates to an instantaneous search through a bank of a finite number of expected observations.

3. Comparison between SDMA Receivers and MUSIC

A simulation was conducted using MATLAB and a comparison was made of the resolution and the accuracy between the SDMA receiver and the MUSIC algorithm. Figure 10 shows the correlation magnitude of SDMA and MUSIC for seven incoming signals with angular separations of 20 degrees. A random array of 31 sensors, occupying

a $25\ \mathrm{m}^2$ rectangular area, was used. All the signals had a carrier frequency of $300\ \mathrm{MHz}$ ($\lambda = 1\ \mathrm{m}$) with a SNR of $15\ \mathrm{dB}$. The results were averaged across 100 Monte Carlo simulations. It is clearly evident that even though the number of signals is large, SDMA provides steep lobes in the directions of the incident signals, while MUSIC gives main lobes which are difficult to identify. Furthermore, SDMA slightly outperforms MUSIC in terms of accuracy as well. Table 1 provides the measured mean value μ and the variance σ^2 in degrees of the average error of two incident angles. Again the results were averaged across 100 Monte Carlo simulations. As expected, both schemes provide unbiased estimates since the mean values are near zero, but SDMA has a slightly smaller variance.

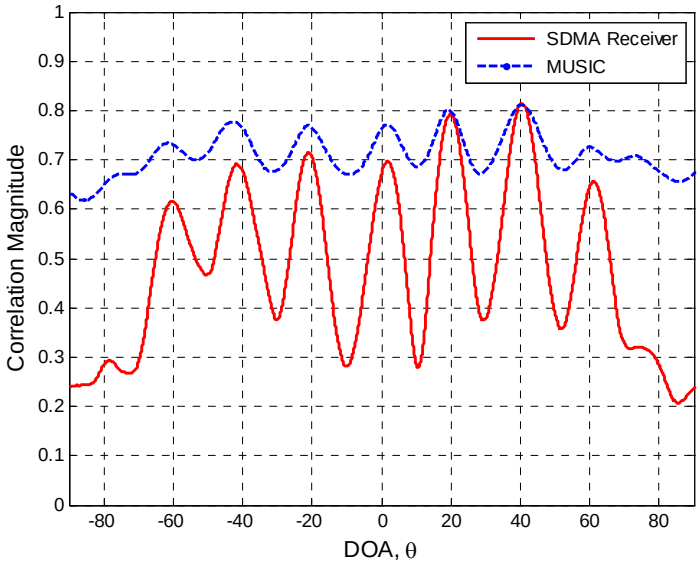

Figure 10. Performance comparison of SDMA and MUSIC for random array of 31 sensors that covers an area of $25\ \mathrm{m}^2$. SNR of incident signals is $15\ \mathrm{dB}$.

	μ	σ^2
MUSIC	0.0917	0.6325
SDMA	-0.015	0.5908

Table 1. Error performance of SDMA and MUSIC.

Using the MATLAB *histfit.m* command, the distribution of the error of both schemes was compared with the theoretical zero-mean Gaussian distribution. The results are shown in Figure 11 for the SDMA receiver and in Figure 12 for the MUSIC algorithm. The results from both schemes can be seen to be closely approximated by the error distribution which is indicated by the red curve in both Figures 11 and 12.

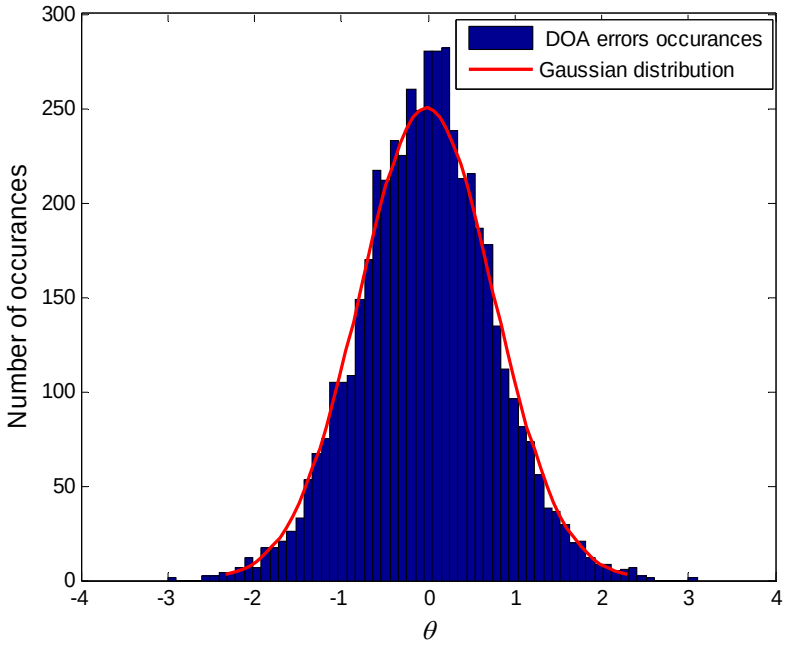

Figure 11. SDMA error distribution.

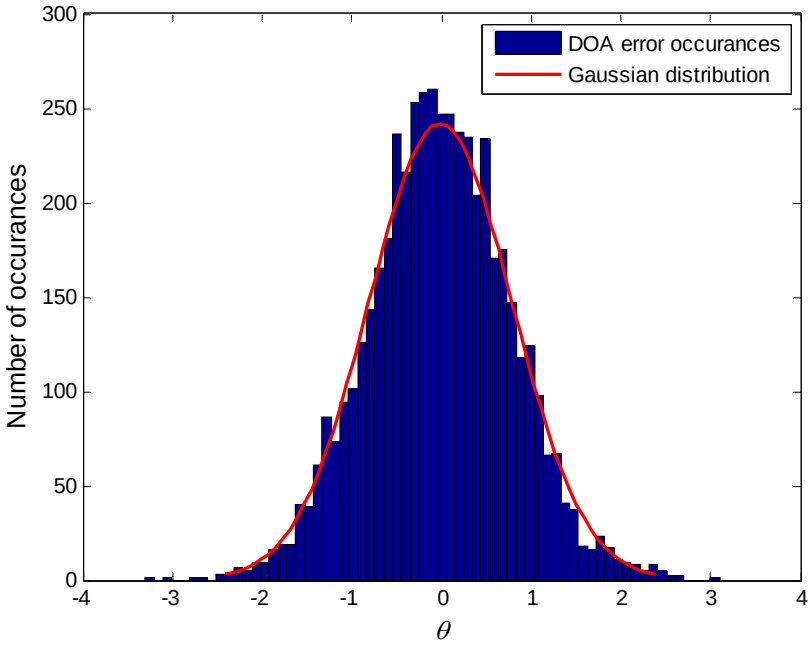

Figure 12. MUSIC error distribution.

Finally, Figure 13 shows the performance of the SDMA receiver and MUSIC in the case of sparse arrays. The same parameters from Figure 10 were used, except that the array area was increased to $2500\ \mathrm{m}^2$. A significant improvement in the resolution of both methods is observed. As discussed earlier, this is an important advantage when using random arrays. The larger spacing between the array elements corresponds to a larger array aperture, which provides higher angular resolution [42]. In the sparse-array case, SDMA is also seen to outperform MUSIC.

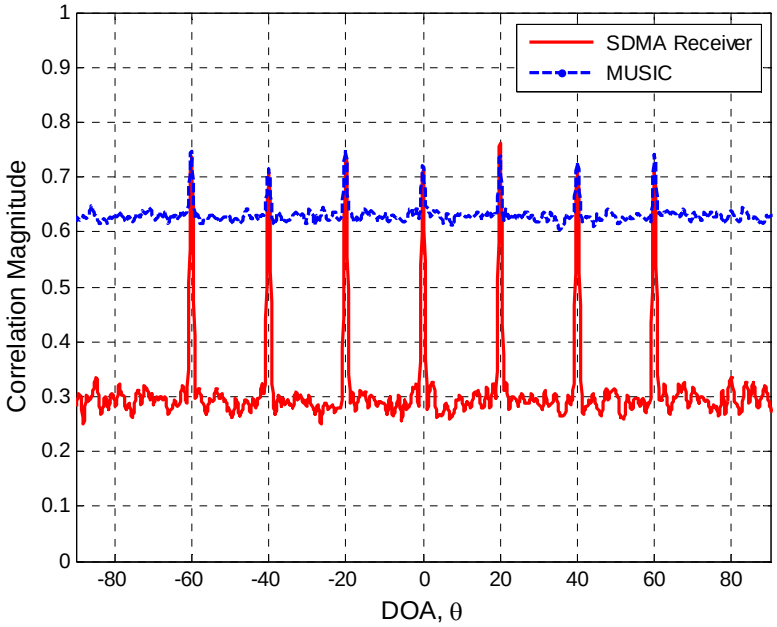

Figure 13. Performance comparison of SDMA and MUSIC for a random array of 31 sensors that covers an area of $2500\ \text{m}^2$. SNR of incident signals is $15\ \text{dB}$.

E. TDOA ESTIMATION

In TDOA-based localization schemes, the first step estimates the time difference of arrival (TDOA) of the incident signal between the sensor nodes in the network. TDOA information can be obtained by two general methods: the first involves the subtraction of the time of arrival between sensors to obtain the relative difference while the second method uses cross-correlation techniques to estimate the desired TDOA [17]. The first method requires knowledge of the transmission time which, in the case of non-cooperative sources, is not available. Accordingly, only the cross-correlation method will be discussed here.

Assume that the signal, $s(t)$, is transmitted by an unknown source. Each sensor in the cluster will receive amplitude-scaled and time-delayed versions of the transmitted signal corrupted by the noise introduced in the channel. Hence, the received signals at two different sensors, $x_1(t)$ and $x_2(t)$, are given by

$$x_1(t) = A_1 s(t-\tau_1) + n_1(t) \text{ and}$$
$$x_2(t) = A_2 s(t-\tau_2) + n_2(t) \tag{37}$$

where A_1 and A_2 are the amplitude scaling factors, $n_1(t)$ and $n_2(t)$ are the additive noise, and τ_1 and τ_2 are the signal offset times at each sensor. A_1 and A_2 reside in the interval $[0,1]$. Assumes that the noise is zero-mean Gaussian and the signal and the noise are uncorrelated. Equation (37) can be rewritten in the form

$$x_1(t) = s(t) + n_1(t)$$
$$x_2(t) = As(t-\tau) + n_2(t) \tag{38}$$

where, without loss of generality, it is assumed that the first sensor is the one with the smaller time of arrival, the amplitudes are normalized by A_1 and τ_1, again without loss of generality, is set to 0. The cross-correlation between the signals $x_1(t)$ and $x_2(t)$ can be approximated by the estimate

$$\hat{R}_{xy}(\tau) = \frac{1}{T}\int_0^T x_1(t)x_2(t-\tau)\,dt \tag{39}$$

where *T* is the time interval during which the observation is conducted. The lag, τ, which maximizes (38) is the estimate of the TDOA value [43].

F. SUMMARY

This chapter provided the background to support the proposed solution for passive source localization of non-cooperative sources. It began by discussing the array response to an incident signal. An overview of the propagation environment followed and a propagation prediction model was adopted to provide a realistic scenario for performance comparison of the localization schemes. It was shown that through a link budget analysis, the signal received by the array can be computed. Finally, the chapter concluded with a discussion of both DOA and TDOA estimation techniques.

In the next chapter we propose a least squares estimator for DOA-based localization. Based on this estimator we develop a hybrid DOA/TDOA localization scheme which exploits both the LOS and the NLOS signals.

THIS PAGE INTENTIONALLY LEFT BLANK

III. PASSIVE SOURCE LOCALIZATION USING RANDOM SENSOR ARRAYS

In this chapter, we address the problem of passive source localization and present the proposed non-cooperative source localization scheme. In the context of random arrays, we begin with an analysis of LOS-only DOA-based localization and then move on to localization using both LOS and NLOS signals.

A. LOS-ONLY DOA-BASED LOCALIZATION

DOA-based localization schemes use DOA estimates of the incident signals to obtain bearings to the position of a source of interest. The bearing estimates are used for the position location determination by triangulation. In a two-dimensional case, there are two unknowns (the coordinates of the source position). In practice, though, more than two bearings are required due to finite angular resolution, multipath fading, and noise [17]. These bearings form an over-determined system of equations which often do not intersect at a single point and can be solved using the least-squares approach. Several proposals exist in literature based on the Least Squared Error (LSE) minimization [18], [45], while others involve the Minimum Mean Square Error estimation or the Maximum Likelihood [46].

1. The Geometry of the Problem

The proposed least squares estimator for DOA localization is based on the geometric configuration of Figure 14. Consider K arrays where each array obtains a DOA estimate by processing the incoming signal from the source. θ_k is the bearing obtained by the array *k*. We begin by formulating the least squares solution of this problem.

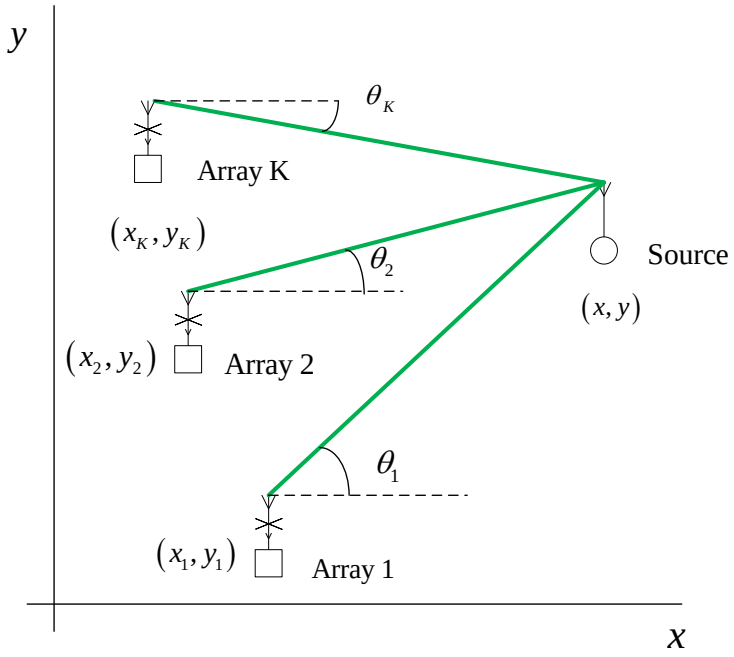

Figure 14. LOS DOA-based source localization using three arrays.

From Figure 14,

$$\tan\theta_k = \frac{y - y_k}{x - x_k}, \tag{40}$$

which can be rewritten as

$$y - x\tan\theta_k = y_k - x_k\tan\theta_k. \tag{41}$$

Doing this for all the arrays yields, in matrix form,

$$\begin{bmatrix} 1 & -\tan\theta_1 \\ 1 & -\tan\theta_2 \\ & \vdots \\ 1 & -\tan\theta_k \end{bmatrix} \begin{bmatrix} y \\ x \end{bmatrix} = \begin{bmatrix} y_1 - \tan\theta_1 x_1 \\ y_2 - \tan\theta_2 x_2 \\ \vdots \\ y_k - \tan\theta_k x_k \end{bmatrix} \tag{42}$$

or

$$A(\theta)\bar{z} = \bar{b}(\theta). \tag{43}$$

2. Least Squares Solution

The matrix $A(\theta)$ in (42) and (43) has a specific structure and is referred as a *Vandermonde matrix*. The solution of least squares problems involving such a matrix is known to be computationally efficient and accurate [47].

a. Least-Squares Estimator

An estimate of the solution to (42) is obtained by minimizing the L_2-norm of the residual [48]

$$\bar{r} = \bar{b}(\theta) - A(\theta)\bar{z}\,. \tag{44}$$

This is graphically depicted in Figure 15 where $\bar{y}$ is the point on the range of A which is closest to $\bar{b}$. From the normal equations, the solution to (42) can be obtained as

$$\bar{z} = A^{+}(\theta)\bar{b}(\theta) \tag{45}$$

where $A^{+}(\theta) = \left[A^{H}(\theta)A(\theta)\right]^{-1} A(\theta)^{H}$ is the pseudo-inverse matrix.

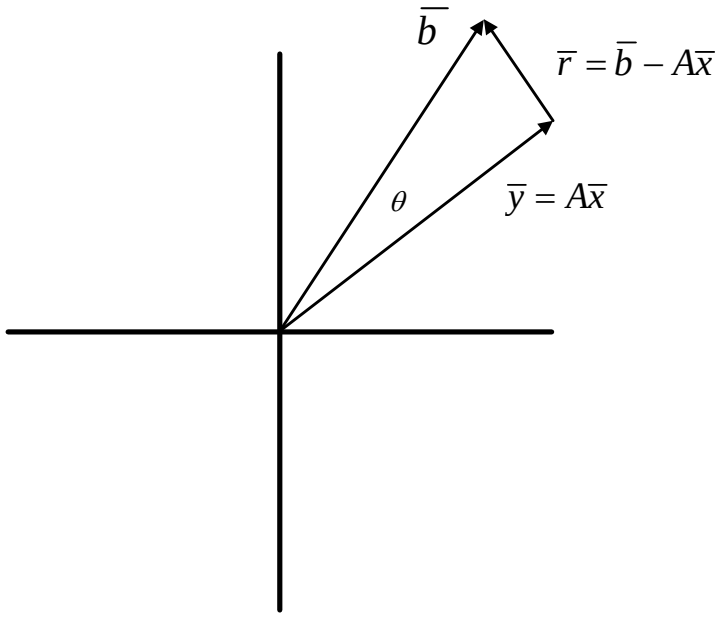

Figure 15. Graphical representation of the least squares problem (From [48]).

b. Statistical Analysis of the Least-Squares Estimator

To show that this estimator is unbiased, let us assume, as discussed previously, that the DOA measurements contain a zero-mean Gaussian error $\delta\bar{\theta}$ such that

$$\bar{\theta}_{est} = \bar{\theta} + \delta\bar{\theta} \,. \tag{46}$$

Correspondingly,

$$A_{est}(\theta) = A(\theta) + \delta A(\theta) \tag{47}$$

and

$$\bar{b}_{est}(\theta) = \bar{b}(\theta) + \delta\bar{b}(\theta) \,. \tag{48}$$

Taking the derivative of both $A(\theta)$ and $\bar{b}(\theta)$ from (42),

$$\frac{dA(\theta)}{d\theta} = \begin{bmatrix} 0 & -\dfrac{1}{\cos^2\theta_1} \\ 0 & -\dfrac{1}{\cos^2\theta_2} \\ & \vdots \\ 0 & -\dfrac{1}{\cos^2\theta_k} \end{bmatrix} \quad \text{and} \quad \frac{d\bar{b}(\theta)}{d\bar{\theta}} = \begin{bmatrix} -\dfrac{x_1}{\cos^2\theta_1} \\ -\dfrac{x_2}{\cos^2\theta_2} \\ \vdots \\ -\dfrac{x_k}{\cos^2\theta_k} \end{bmatrix}. \tag{49}$$

Using the approximations $\delta\theta \approx d\theta$, $\delta\bar{b} \approx d\bar{b}$ and $\delta A \approx dA$,

$$\delta A = \begin{bmatrix} 0 & -\dfrac{\delta\theta_1}{\cos^2\theta_1} \\ 0 & -\dfrac{\delta\theta_2}{\cos^2\theta_2} \\ & \vdots \\ 0 & -\dfrac{\delta\theta_k}{\cos^2\theta_k} \end{bmatrix} \quad \text{and} \quad \delta\bar{b} = \begin{bmatrix} -\dfrac{\delta\theta_1 x_1}{\cos^2\theta_1} \\ -\dfrac{\delta\theta_2 x_2}{\cos^2\theta_2} \\ \vdots \\ -\dfrac{\delta\theta_k x_k}{\cos^2\theta_k} \end{bmatrix}. \tag{50}$$

Substituting (47) and (48) into (43)

$$\left(A + \delta A\right)^T \left(\bar{b} + \delta\bar{b}\right) = \left(A + \delta A\right)^T \left(A + \delta A\right)\left(\bar{z} + \delta\bar{z}\right) \tag{51}$$

where $\delta\bar{z}$ is the error in the source location estimation. Expanding (51) and ignoring the second order terms,

$$A^T\bar{b} + A^T\delta\bar{b} + \delta A^T\bar{b} = A^T A\bar{z} + A^T\delta A\bar{z} + \delta A^T A\bar{z} + A^T A\delta\bar{z}\ .$$

Rearranging terms,

$$A^T\left(\delta\bar{b} - \delta A\bar{z}\right) + \left(A^T + \delta A^T\right)\left(\bar{b} - A\bar{z}\right) = A^T A\delta\bar{z}\ .$$

With $\bar{b} - A\bar{z} = 0$, reduces to

$$\left(A^T A\right)^{-1} A^T\left(\delta\bar{b} - \delta A\bar{z}\right) = \delta\bar{z}.$$

Using the pseudoinverse we finally arrive at

$$\delta\bar{z} = A^{+}\left(\delta\bar{b} - \delta A\bar{z}\right) \tag{52}$$

which has the expectation

$$E\left\{\delta\bar{z}\right\} = A^{+}E\left\{\delta\bar{b} - \delta A\bar{z}\right\}. \tag{53}$$

The vector inside the expectation of (53) is

$$\delta\bar{b} - \delta A\bar{z} = \begin{bmatrix} \dfrac{\left(x - x_1\right)}{\cos^2\theta_1}\delta\theta_1 \\ \dfrac{\left(x - x_2\right)}{\cos^2\theta_2}\delta\theta_2 \\ \vdots \\ \dfrac{\left(x - x_k\right)}{\cos^2\theta_k}\delta\theta_k \end{bmatrix} \tag{54}$$

and has a mean value of

$$E\left\{\delta\bar{b} - \delta A\bar{z}\right\} = \begin{bmatrix} \dfrac{\left(x - x_1\right)}{\cos^2\theta_1}E\left\{\delta\theta_1\right\} \\ \dfrac{\left(x - x_2\right)}{\cos^2\theta_2}E\left\{\delta\theta_2\right\} \\ \vdots \\ \dfrac{\left(x - x_k\right)}{\cos^2\theta_k}E\left\{\delta\theta_k\right\} \end{bmatrix}. \tag{55}$$

However, $E\left\{\delta\theta_k\right\} = 0$ for every $k \in \left(1, K\right)$ since the DOA error is zero-mean and, therefore, $E\left\{\delta\bar{b} - \delta A\bar{z}\right\} = 0$. From (53), it follows that $E\left\{\delta\bar{z}\right\} = 0$ and the proposed estimator is unbiased.

The accuracy of the proposed scheme, and of that of any DOA-based localization scheme, is affected by the error in DOA estimation. A metric of the accuracy of these schemes can be explained in terms of the covariance matrix [49]

$$C_{\bar{z}} = \left(A^H C_{\bar{\theta}}^{-1} A \right)^{-1} \tag{56}$$

where $C_{\bar{\theta}} \in \mathbb{C}^{K \times K}$ is the covariance matrix of the DOA error estimates (assumed to be zero mean white noise sequence in this case). $C_{\bar{\theta}}$ is a diagonal matrix and each element along the main diagonal represents the error variance of the measured DOA for the corresponding array. If the statistics of the error sequence are known and each array has a different noise variance, appropriate weighting of the least-squares solution leads to an optimum estimator [49]. The weighting matrix is chosen to be the $C_{\bar{\theta}}^{-1}$ and the general form of the weighted least-squares estimator is

$$\bar{x}_{est} = \left(A^H C_{\bar{\theta}}^{-1} A \right)^{-1} A^H C_{\bar{\theta}}^{-1} \bar{b} \, . \tag{57}$$

c. Conditioning of the Least-Squares Solution

The conditioning of the least-squares problem captures the perturbation behavior of the least-squares solution [47]. A least-squares problem is characterized as either well-conditioned or ill-conditioned. An ill-conditioned problem is one in which a small perturbation in the observed data leads to a large error in the estimated solution and the condition number is a metric used to quantify the conditioning. A well-conditioned problem has a condition number equal to one. As the condition number increases, the problem becomes increasingly ill-conditioned.

In the least-squares problem of (42), the condition numbers which describe the solution $\bar{z}$, with respect to the perturbations of the matrix A and the vector $\bar{b}$ as shown in Figure 15, are given by the equations of Table 2 [47] where

$$\kappa(A) = \frac{\sigma_1}{\sigma_2}, \quad 1 \le \kappa(A) < \infty \quad ,$$

$$\theta = \cos^{-1} \frac{\left\| \bar{y} \right\|}{\left\| \bar{b} \right\|} \, , \; 0 \le \theta \le \frac{\pi}{2} \quad ,$$

$$\eta = \frac{\|A\|\|\bar{z}\|}{\|\bar{y}\|}, \quad 0 \le \eta \le \kappa(A)$$

and σ_1 and σ_2 are the maximum and the minimum singular values of A, respectively. Here, the rank of the matrix A is 2 and, therefore, two singular values exist. The conditioning of the least-squares problem clearly depends on the geometry of the specific scenario under consideration.

	Condition number
$\bar{b}$	$\frac{\kappa(A)}{\eta \cos\theta}$
A	$\kappa(A) + \frac{\kappa(A)^2 \tan\theta}{\eta}$

Table 2. Condition numbers of the least-squares problem [From 47].

d. Geometric Dilution of Precision

The geometry formed by the arrays which participate in the localization procedure and the source of interest affects the accuracy of the estimated source position [5]. As the distance between the source and the baseline increases relative to the length of the baseline, the accuracy of the least-squares solution decreases. This is because larger relative distances correspond to smaller differences in bearings at the arrays. Thus, relatively large source distances increase the condition number of matrix A and tend to make it singular. This, in turn, affects the stability of the least-squares problem. This phenomenon is called geometric dilution of precision and is illustrated in Figure 16. As the relative distance of the source from the baseline is increased, the uncertainty area, formed by the intersections of the estimated bearings is also increased. Furthermore, the angle between the orthogonal bisection of the baseline and the bearing to the source from the midpoint of the baseline also affects the accuracy of the solution. As illustrated in Figure 17, as angle θ_{BS} increases, the uncertainty area becomes larger.

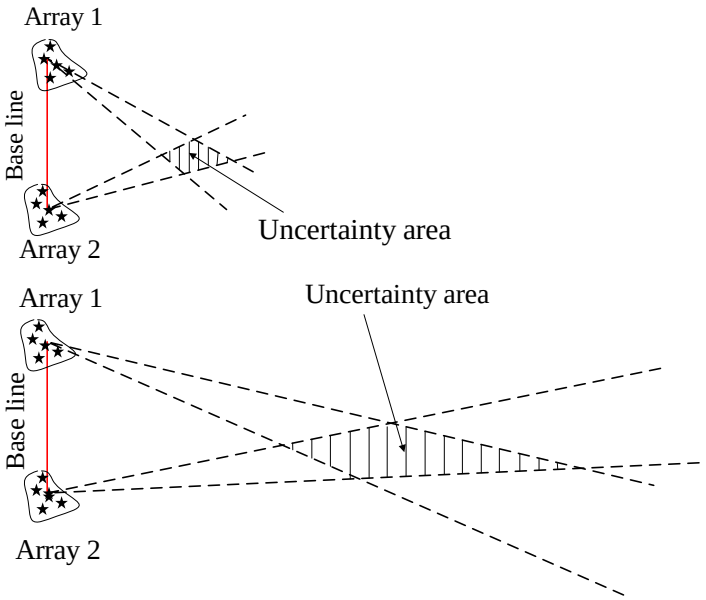

Figure 16. The effect of distance to the source on the geometric dilution of the precision.

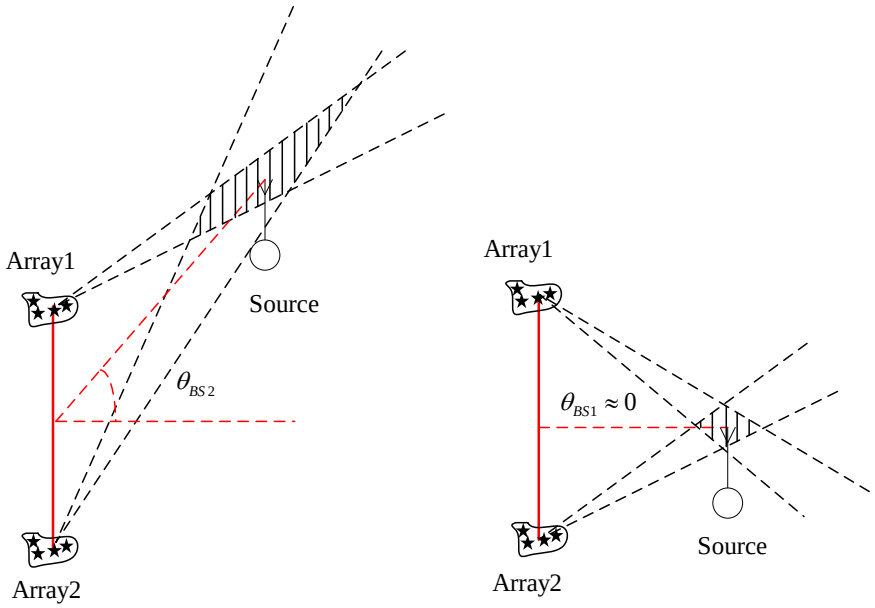

Figure 17. The effect of the bearing to the source on geometric dilution of the precision.

3. Total Least Squares

In the proposed least squares estimator, both A and $\bar{b}$ can be affected by errors. For a least-squares problem, the total least squares (TLS) method is known to compensate for errors in matrix A [49]. Let $C = \begin{bmatrix} A & \bar{b} \end{bmatrix}$ with $C \in \mathbb{C}^{k\times 3}$. The singular value decomposition of matrix C is

$$C = U\Sigma V^H \tag{58}$$

where $U \in \mathbb{C}^{k\times 3}$, $\Sigma \in \mathbb{R}^{3\times 3}$ and $V \in \mathbb{C}^{3\times 3}$. Matrices U and V are unitary and Σ is a diagonal matrix of the form

$$\Sigma = \begin{bmatrix} \sigma_{1C} & 0 & 0 \\ 0 & \sigma_{2C} & 0 \\ 0 & 0 & \sigma_{3C} \end{bmatrix} \tag{59}$$

where its diagonal elements are the singular values of C, satisfying $\sigma_{1C} \geq \sigma_{2C} \geq \sigma_{3C}$. The TLS solution of the least-squares problem using the total least-squares estimator can then be shown to be [49]

$$\bar{x}_{TLS} = \left(A^H A - \sigma_{3C}\mathrm{I}\right)^{-1} A^H \bar{b} \,. \tag{60}$$

A simulation was conducted in MATLAB to compare the performance of the proposed model using both the LS and the TLS methods. The DOA estimation error was assumed to be zero-mean Gaussian with a standard deviation of 0.5 degrees. The results are shown in Figure 18 as a function of the number of sensor arrays. The LS solution can be seen to outperform the TLS solution for small numbers of arrays, while the TLS solution is slightly better for 10 arrays or more.

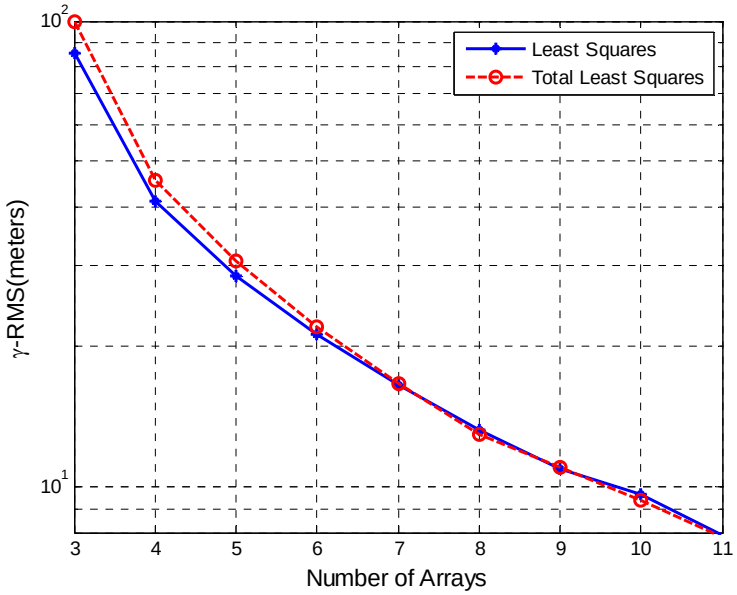

Figure 18. RMS error for LS vs. TLS for 1000 Monte Carlo simulations with $\sigma_{DOA} = 0.5°$.

These results are surprising and contradict existing literature. As mentioned in [49], the TLS is a deregularizing procedure. The conditioning of the TLS problem should always be worse than the conditioning of the respective LS problem. The ratio of the smallest singular value of A to the smallest singular value of C has been defined as a metric to quantify the instability of the TLS and to indicate whether the LS outperforms the TLS [49]. As this ratio, $\frac{\sigma_{2A}}{\sigma_{3C}}$ in this case, approaches unity, the TLS tends to be unstable and the LS solution performs better. This ratio was computed for the simulation of Figure 18 and is shown in Table 3. The results can be seen to agree with the performance of the TLS algorithm.

Arrays	3	4	5	6	7	8	9	10	11
$\frac{\sigma_{2A}}{\sigma_{3C}}$	5.4513	5.4934	6.3222	6.9740	7.8332	8.9594	9.9635	11.0359	12.0155

Table 3. Stability measure for the TLS algorithm.

4. Sequential Least Squares

As time progresses, more incoming signal samples may arrive at the array from the same source. Hence, more data will be available and, by exploiting it, the estimate of the source location can be improved. In this case the localization procedure becomes a dynamic task and an algorithm which continuously updates the information matrices is needed [48]. If the noise is uncorrelated (which implies that the covariance matrix $C_{\bar{\theta}}$ is diagonal), then A can be computed sequentially as

$$A[k] = \begin{bmatrix} A[k-1] \\ \bar{a}^H[k] \end{bmatrix} \tag{61}$$

where $A[k]$ is the data matrix of k measurements, $A[k-1]$ is the $k \times 2$ matrix of the previous $k-1$ measurements and $\bar{a}^H[k]$ is the k^{th} measurement. Recall that $\bar{a}^H[k] = [1 \quad \tan\theta_k]$ for the proposed scheme. Thus, the sequential estimator is [48]

$$\bar{z}[k] = \bar{z}[k-1] + D[k]\left(b[k] - \bar{a}^H[k]\bar{z}[k-1]\right) \tag{62}$$

where

$$D[k] = \frac{C_{\bar{\theta}}[k-1]\bar{a}[k]}{\sigma^2{}_k + \bar{a}^H[k]C_{\bar{\theta}}[k-1]\bar{a}[k]} \tag{63}$$

and the covariance update is given as

$$C_{\bar{\theta}}[k] = \left(I - D[k]\bar{a}^H[k]\right)C_{\bar{\theta}}[k-1]. \tag{64}$$

B. LOS AND NLOS DOA-BASED LOCALIZATION

The proposed hybrid DOA/TDOA LOS and NLOS localization scheme is implemented in three steps. A block diagram of the proposed scheme is shown in Figure 19. The first step implements the DOA estimation using the SDMA receiver as described in the previous chapter. A detailed description of steps 2 and 3 (bearing association and source localization, respectively) are included in the following subsections.

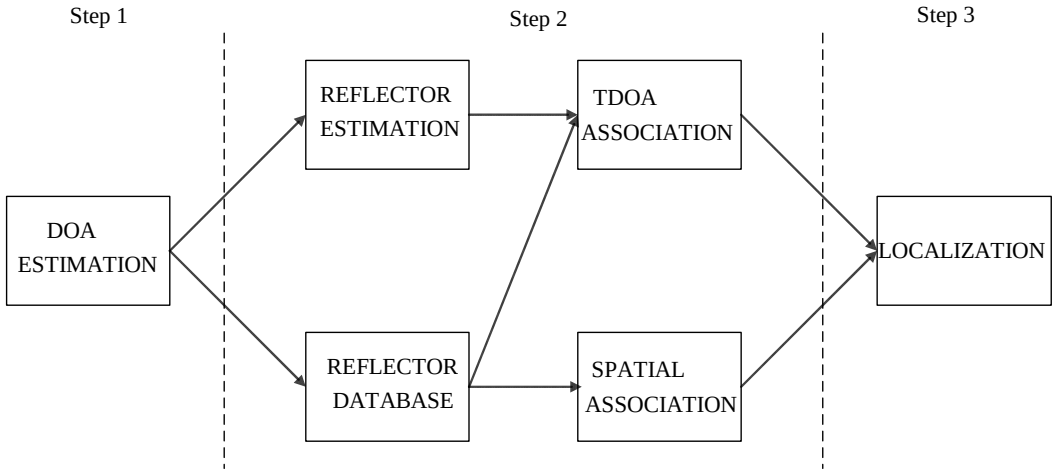

Figure 19. Block diagram of the proposed LOS and NLOS localization scheme.

1. Association of Bearings

Once the DOAs have been determined for the incident signals, they are then associated with each other according to source-reflector pairs. Specifically, for each source-reflector pair, a LOS and a NLOS is identified based on knowledge of the reflector position and geometry. This reflector knowledge can be obtained either from static databases which contain the footprint of the large objects within the environment under consideration [21] or dynamically by sending a beacon from a known location and using the reflector position estimation algorithm which is described in the following subsection. When neither of these tools is available, the proposed scheme is capable of performing reflector position estimation. In this case, the problem becomes one in which the scheme simultaneously performs both reflector mapping and source localization. In the remainder of this section, we begin with a discussion of how this reflector mapping is accomplished and then present the association scheme.

a. Reflector Position Estimation

To discuss the reflector mapping algorithm, consider Figure 20 where a single source transmits a narrowband signal and N reflectors generate NLOS signals that can be viewed as secondary sources. A minimum of three arrays must be available to solve the reflector estimation problem. Let $\theta_{i,n}$ be the bearing associated with array i and

reflector n and $\theta_{i,s}$ the LOS bearing from source S to array i. The bearing correspondences can be illustrated with a $(N+4, 3N+3)$-bipartite graph as shown in Figure 21. There are $N+4$ vertices in the graph and $3N+3$ edges. The number of edges corresponds to the total number of bearings. The interrelationship between the bearings is determined in two steps as shown in Figure 22. In the first step, all the intersections between the bearings of array 1 and array 2 are found. In this step, a total of $(N+1)^2$ 2×2 systems of equations are solved. In step two, the residuals between those points and the bearings of array 3 are computed. The $N+1$ smaller residuals indicate which intersections of array 1 and array 2 bearings correspond to which bearing of array 3. This second step involves the solution of $(N+1)^3$ equations. Thus, the total number of required operations grows as N^3. The source and the image sources related to the reflectors are estimated by solving for the interrelated bearings using the least squares estimator of the proposed scheme. The orientation and the position of reflector n according to Figure 20 is then given as

$$\bar{z}_n = \begin{bmatrix} \dfrac{y + y'_{Rn}}{2} \\ \dfrac{x + x'_{Rn}}{2} \end{bmatrix} \tag{65}$$

with

$$\theta_n = \begin{cases} 0^\circ & x = x'_{Rn} \\ \arctan\left(\dfrac{y'_{Rn} - y_s}{x'_{Rn} - x_s}\right) - 90^o & x \neq x'_{Rn} \end{cases} \tag{66}$$

.

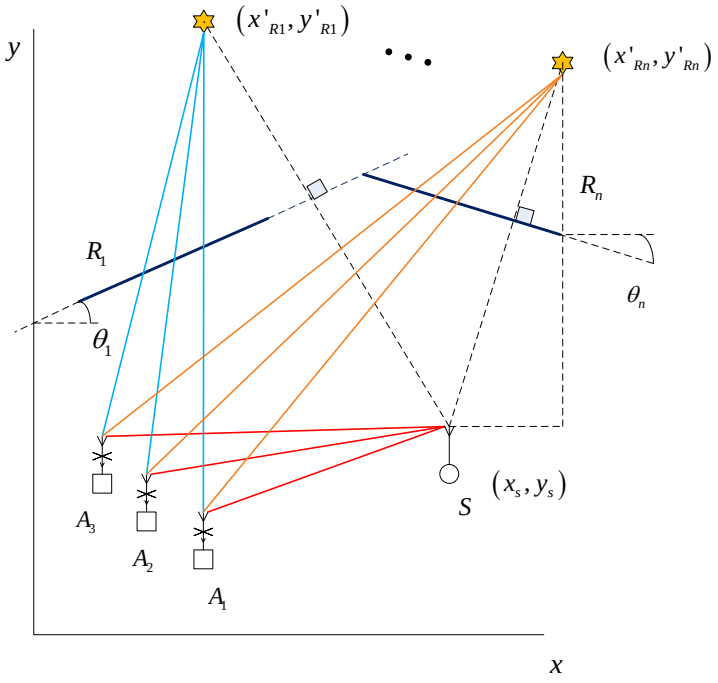

Figure 20. Unknown reflector position and orientation estimation with three arrays.

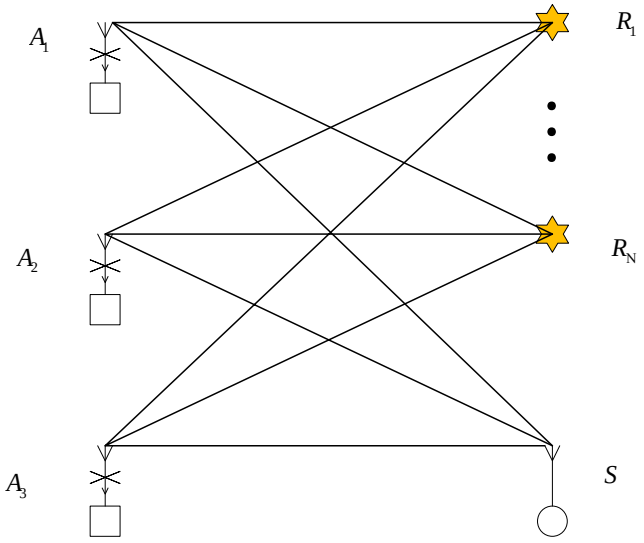

Figure 21. Representation with a $(N+4, 3N+3)$ biparte graph of the bearing correspondences of the reflector source pairs for N reflectors.

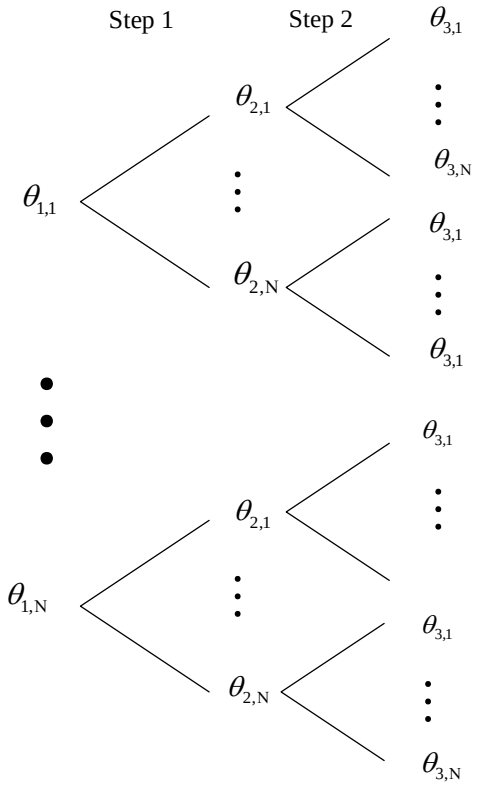

Figure 22. Two-step procedure for finding the bearing correspondences of the reflector source pairs

b. Bearing Association using Expected TDOA Estimation

Once the positions of the reflectors have been determined, each array can associate its bearings using a set of time markers. From Figure 23 and using the sinusoids law,

$$\frac{d_{INC}}{\sin(\theta_R - \theta_L)} = \frac{d_{REF}}{\sin(\theta_R + \theta_L - 2\theta_o)} = \frac{d_{LOS}}{\sin(2\theta_R - 2\theta_o)}. \tag{67}$$

where $d_{AA'}$ is the distance between the array and its image (with respect to the reflector), θ_o is the orientation of the reflector, θ_L is the LOS bearing and θ_R is the NLOS bearing. However,

$$\Delta d = d_{LOS} - d_{INC} - d_{REF} \tag{68}$$

and, combining (67) and (68),

$$\Delta d = \frac{\sin\left(2\theta_R - 2\theta_o\right) - \sin\left(\theta_R + \theta_L - 2\theta_o\right) - \sin\left(\theta_R - \theta_L\right)}{\sin\left(\theta_R + \theta_L - 2\theta_o\right)} d_{REF} \,. \tag{69}$$

We also note that

$$d_{REF} = \frac{d_{AA'}}{2\sin\left(\theta_R - \theta_o\right)} \quad \text{and} \quad \Delta\tau = \frac{\Delta d}{c} \tag{70}$$

where c is the propagation speed and $\Delta\tau$ is the desired expected TDOA between the LOS and the NLOS signals. Substituting (69) into (70) the expression for $\Delta\tau$ is

$$\Delta\tau = \frac{\varphi}{\sin\left(\theta_R + \theta_L - 2\theta_o\right)\sin\left(\theta_R - \theta_o\right)}\left(\frac{d_{\mathrm{AA'}}}{2c}\right) \tag{71}$$

where

$$\begin{aligned} \varphi = &\sin\left(2\theta_R - 2\theta_o\right) \\ &- \sin\left(\theta_R + \theta_L - 2\theta_o\right) - \sin\left(\theta_R - \theta_L\right) \end{aligned} \tag{72}$$

The TDOAs for all combinations of ordered pairs of bearings are solved using (71) for each reflector to give the complete set of possible expected TDOAs which can be shown to number

$$2N\binom{M\left(N+1\right)}{2} = M^2\left(N^3 + 2N^2 + N\right) - M\left(N^2 + N\right) \tag{73}$$

TDOAs where M is the number of transmitting sources. It should be emphasized that this set is derived using the DOA estimations from the first step of the proposed scheme.

The set of expected TDOAs is compared with the observed TDOAs, which have been calculated from the time markers using a weighted version of the generalized cross correlation estimator. For a given source, the bearing association is then accomplished by matching ordered pairs of the expected TDOAs to the observed TDOAs.

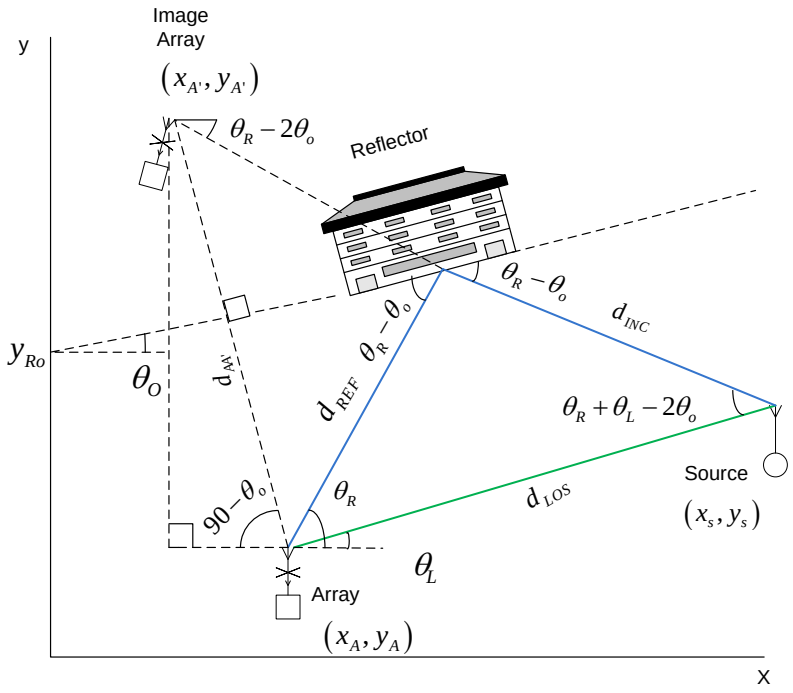

Figure 23. Single-array, single-source, single-reflector scenario used to illustrate the expected TDOA relationship between the LOS and the NLOS signal.

c. Spatial Bearing Association

As depicted in Figure 24, when a single source is considered and the exact footprint of the reflectors is known, the association problem can be solved spatially without the need of TDOA estimation. This saves processing load which is desirable in wireless sensor network applications. For the single reflector scenario, two cases can be identified. In the first, one bearing is outside of the sector defined between the reflector and the array as in Figure 24(a). This bearing can be clearly identified as the LOS signal. In the second case, both bearings reside inside the sector as in Figure 24(b). In this case, the localization problem (discussed in the next section) is solved twice for each of the potential LOS bearings. These solutions will generate two distinct points. One is the position of the source while the second is an image of the source related to the specific reflector. The latter point can be readily determined to be unrealistic based on the known location of the reflector and the former is identified as the actual position of the source.

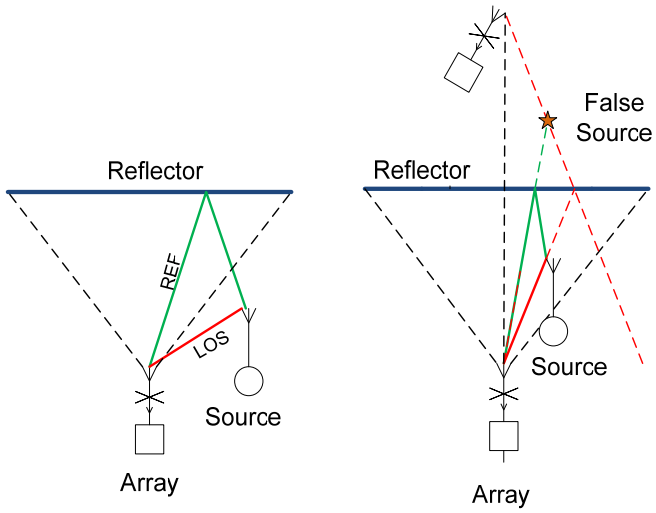

Figure 24. Spatial bearing association when one source transmits and the exact footprint of the reflector is known.

When multiple reflectors are considered, each one defines an independent sector and, in the case where a sector contains two bearings, the association can be solved as above. When each sector contains at most one bearing, then the least squares localization problem described in the next section is solved as many times as the number of the bearings by considering a different bearing as the LOS each time. The least squares formulation, which converges to a solution, simultaneously solves both the association problem and the localization problem. If no solution results from the procedure, then no LOS signal exists and the localization problem is solved by considering all bearings as NLOS.

In the preceding discussion, it is assumed that all reflections are “single bounce.” This is a reasonable assumption provided a signal strength threshold is used at each receiver.

2. Localization using both LOS and NLOS Signals

The third step in the proposed scheme is the source localization algorithm itself. In this section, we begin by describing the single array case and then expand the localization procedure to the multiple arrays case. For the latter, we propose both centralized and distributed solutions.

a. Single Array Localization

As we have noted earlier, the proposed scheme is capable of providing single array localization. As shown in Figure 25, if at least one NLOS bearing is available, the source position is found as the intersection of the LOS bearing and the bearing with angle $2\theta_o - \theta_R$ with respect to the image array. This image array is defined in a similar manner to the image source described earlier and its position is given by

$$\overline{z}_{A'} = \begin{bmatrix} x_{A'} \\ y_{A'} \end{bmatrix} = \begin{bmatrix} 2x_{RA} - x_A \\ 2y_{RA} - y_A \end{bmatrix}. \tag{74}$$

We also note that

$$y_{RA} = \tan\theta_o x_{RA} + y_{Ro} \tag{75}$$

and

$$\tan\left(90 - \theta_o\right) = \frac{y_{RA} - y_A}{x_A - x_{RA}}. \tag{76}$$

Combining (75) and (76), we see that

$$x_{RA} = \frac{1}{1+\tan^2\theta_o} x_A + \frac{\tan\theta_o}{1+\tan^2\theta_o}\left(y_A - y_{Ro}\right) \tag{77}$$

and

$$y_{RA} = \frac{\tan\theta_o}{1+\tan^2\theta_o} x_A + \frac{\tan^2\theta_o}{1+\tan^2\theta_o}\left(y_A - y_{Ro}\right). \tag{78}$$

Substituting (77) and (78) into (74), we have

$$\overline{z}_{A'} = \begin{bmatrix} \dfrac{\left(1-\tan^2\theta_o\right)x_A + 2\tan\theta_o\left(y_A - y_{Ro}\right)}{1+\tan^2\theta_o} \\ \dfrac{2\tan\theta_o x_A + \left(2\tan^2\theta_o - 1\right)y_A - 2\tan^2\theta_o y_{Ro}}{1+\tan^2\theta_o} \end{bmatrix}. \tag{79}$$

Using (42), the least squares formulation of the single array localization problem when a single NLOS signal exists in conjunction with the LOS signal is

$$A=\begin{bmatrix}1 & -\tan\theta_L \\ 1 & -\tan\left(2\theta_o-\theta_R\right)\end{bmatrix}, \tag{80}$$

$$\bar{b}=\begin{bmatrix} y_{\mathrm{A}}-\tan\theta_L x_{\mathrm{A}} \\ y_{\mathrm{A'}}-\tan\left(2\theta_o-\theta_R\right)x_{\mathrm{A'}}\end{bmatrix}. \tag{81}$$

When the reflections of at least two reflectors are present the localization task can be performed by using only the NLOS signals. Considering the scenario of Figure 25, matrix A and the corresponding vector $\bar{b}$ in (42) become

$$A=\begin{bmatrix}1 & -\tan\left(2\theta_{o1}-\theta_{R1}\right) \\ 1 & -\tan\left(2\theta_{o2}-\theta_{R2}\right)\end{bmatrix},\quad \bar{b}=\begin{bmatrix} y_{\mathrm{A1'}}-\tan\left(2\theta_{o1}-\theta_{R1}\right)x_{\mathrm{A1'}} \\ y_{\mathrm{A1'}}-\tan\left(2\theta_{o1}-\theta_{R1}\right)x_{\mathrm{A1'}}\end{bmatrix}. \tag{82}$$

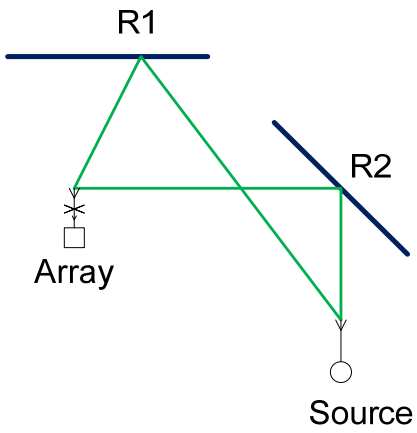

Figure 25. Single-array NLOS-only localization with two reflectors.

b. Proposed Multiple-Array Centralized Localization Scheme

Consider the multiple array-multiple reflector scenario of Figure 26 in which K arrays have available the NLOS reflections from N reflectors. This problem is over-determined and can be solved using the least-squares estimator proposed earlier. The formulation of the matrix A and the corresponding vector $\bar{b}$ is

$$A=\begin{bmatrix} A_1 \\ A_2 \\ \vdots \\ A_K \end{bmatrix}, \quad \bar{b}=\begin{bmatrix} \bar{b}_1 \\ \bar{b}_2 \\ \vdots \\ \bar{b}_K \end{bmatrix} \tag{83}$$

where $A_k \in \mathbb{C}^{(N+1)\times 2}$ is the matrix of data obtained by the k^{th} array and $\bar{b}_k \in \mathbb{C}^{N+1}$ is the corresponding vector. These can be shown to be

$$A_k=\begin{bmatrix} 1 & -\tan\theta_{L_k} \\ 1 & -\tan\left(2\theta_{o_1}-\theta_{A_{k1}}\right) \\ & \vdots \\ 1 & -\tan\left(2\theta_{o_n}-\theta_{A_{kn}}\right) \end{bmatrix} \text{ and } \quad \bar{b}_k=\begin{bmatrix} y_{A_k}-\tan\theta_{L_k}x_{A_k} \\ y_{A'_{k1}}-\tan\left(2\theta_{o_1}-\theta_{A_{k1}}\right)x_{A'_{k1}} \\ \vdots \\ y_{A'_{kn}}-\tan\left(2\theta_{o_n}-\theta_{A_{kn}}\right)x_{A'_{kn}} \end{bmatrix}. \tag{84}$$

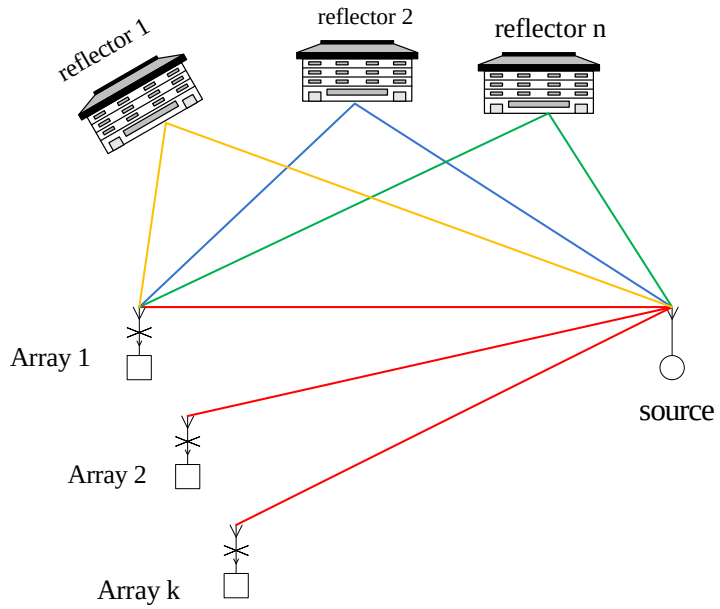

Figure 26. Single-source localization using multiple arrays in the presence of multiple reflectors.

This localization scheme is a centralized scheme which involves a data fusion center to process the incoming data collected by the arrays. In a WSN, the fusion center may be an array of sensors as well. The centralized approach has several fundamental drawbacks when implemented in WSNs. The most important is the

increased energy consumption of the fusion center. Thus, the array assigned to act as the fusion center will have a shorter lifetime due to the added processing and communication load which will affect the lifetime of the entire WSN.

c. Proposed Multiple-Array Distributed Localization Scheme

As an alternative to the centralized approach above, a distributed solution can be implemented that solves the localization problem for each single array individually and then averages the individual array estimates. A two-step approach, this solution is summarized in Figure 27. This distributed approach is of particular interest in wireless sensor network deployments since it distributes the processing load among multiple sensor nodes and reduces the communication burden which is the primary energy consumer [2].

Step 1: Single array localization.

$$\overline{z}_k = \left(A_k{}^H A_k \right)^{-1} A_k{}^H \overline{b}_k \qquad \text{for } k = 1:K$$

Step 2: Estimated position averaging.

$$\overline{z} = \frac{1}{K} \sum_{k=1}^{K} \overline{z}_k$$

Figure 27. Proposed distributed localization scheme.

C. SUMMARY

In this chapter, we proposed a least squares estimator for DOA-based localization which is unbiased when the noise is Gaussian-distributed with zero mean. This estimator solves an over determined Vandermonde system of equations which is known to be computationally efficient and accurate.

Based on this least squares error estimator, we proposed a passive source localization scheme which exploits the NLOS signals from non-cooperative sources. The proposed solution is a hybrid DOA/TDOA source localization scheme and is comprised of three parts: a DOA estimator, an association algorithm for the identified signal bearings, and the source localization scheme itself. The recently proposed Space Division

Multiple Access (SDMA)-based receiver was used for DOA estimation. TDOA information was used to discriminate between the line-of-sight (LOS) and the NLOS signals and to associate the incoming multipath signal with the corresponding source and reflector pair. It was shown that, in special cases, the proposed scheme is capable of solving the association problem spatially without the need for TDOA information. A technique was also provided to estimate the position and the orientation of the reflectors when site-specific database information is not available. Both centralized and distributed variants of the proposed scheme were presented with the latter being of particular interest in WSNs.

In the next chapter, we evaluate the performance of the proposed passive source localization scheme using MATLAB.

THIS PAGE INTENTIONALLY LEFT BLANK

IV. SIMULATION RESULTS OF THE PROPOSED LOCALIZATION SCHEME

In this chapter, simulation results are provided to validate the performance of the proposed localization scheme. We begin with a discussion of the MATLAB simulation code, the supporting link budget analysis, and the performance metrics. Following this, simulation results are provided and analyzed for both the single reflector and the multiple reflector cases.

A. SET-UP OF THE SIMULATION

The performance of the proposed localization scheme is validated using the MATLAB simulation environment. Details of the underlying simulation are provided in the following subsections.

1. Matlab Simulation

The MATLAB code used in this thesis is included in the Appendix and is implemented in three steps according to the block diagram of Figure 19. The operational scenario simulated in MATLAB contains one source and two reflectors with a narrowband signal is transmitted at a given SNR from the source. The propagation environment is modeled as discussed in Chapter II and a link budget analysis is conducted. The incident signal at the arrays is processed and the response of each array is given by the function resignal.m. The SDMA receiver is simulated with the MATLAB function doa_sdma.m. Once the DOA estimations have been determined, the simulation associates the reflector-source bearing pairs and performs the localization. Finally, the MATLAB code simulates and compares the LOS-only localization scheme and the proposed localization scheme which utilizes both LOS and NLOS signals.

2. Environment Simulation and Link Budget Analysis

Using the scenario shown in Figure 28, we now provide an example link budget analysis. This single-source, single-reflector example can be expanded to scenarios with multiple reflectors or sources. The source transmits a narrowband signal with 30 kHz

bandwidth at a carrier frequency of 300 MHz. The signal is received at the array via two multipath components. The first path is the LOS, while the second is a "single bounce" NLOS signal. The power of the transmitted signal is 0.1 mW. The source is located at coordinates $(x_S, y_S) = (170\text{ m}, 230\text{ m})$, while the array is at the origin. The reflector has orientation $\theta_1 = 10^o$ with respect to the x-axis. The reference point y_R is located at $(0\text{ m}, 400\text{ m})$. The angle $\theta_L = 45°$ corresponds to the DOA of the LOS path, while $\theta_R = 79.48°$ is the DOA of the reflection. The length of the LOS path is 282.84 m, while the length of the NLOS path is 667.08 m. Each individual array contains 50 sensors randomly distributed in an area of size $15\text{ m} \times 15\text{ m}$.

Assuming a system temperature of 400 K, the transmitted signal SNR is equal to117.81 dB. The received SNRs for the LOS and the NLOS components are 64.93 dB and 49.24 dB, respectively. The NLOS path is weaker than the LOS path by 15.69 dB. As expected, this is the result of a longer propagation path combined with the reflection loss.

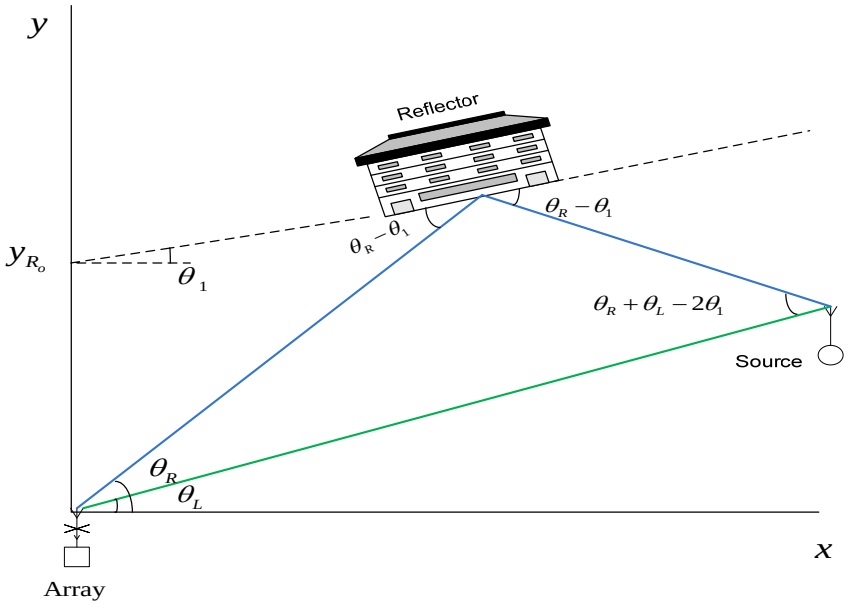

Figure 28. Single-source, single-reflector scenario used in the reported link budget analysis.

3. Performance Metrics

We model three uncertainties in the simulation scenarios. The first is introduced by the noise of the received signal which is considered zero-mean Gaussian. A second is generated by the uncertainty in the position of the sensors within the arrays. Finally, the different arrays are randomly distributed in the specified area. To capture the performance of our proposed scheme, we define a metric based on an estimation $\bar{r}$ of the distance of the source from the array r and given as

$$\gamma_r = \sqrt{\sigma_r^2 + \mu_r^2} \quad \text{(RMS error)} \tag{85}$$

where

$$\mu_r = \frac{1}{P}\sum_{i=1}^{M}\left(\bar{r} - r\right) \quad \text{(mean error)}, \tag{86}$$

$$\sigma^2{}_r = \frac{1}{P}\sum_{i=1}^{M}\left(\bar{r} - \mu_r\right)^2 \quad \text{(error variance)} \tag{87}$$

and P is the number of Monte Carlo simulations.

B. SIMULATION RESULTS OF THE PROPOSED LOCALIZATION SCHEME

In this section, simulation results are provided to evaluate the performance of the proposed scheme. In the first subsection, we examine the case of a single-source, single-reflector. In the second subsection, we extend this to multiple reflectors.

In the following discussion, the term known reflector implies that the knowledge was obtained from existing databases or by a beacon, while the term unknown reflector means that the position of the reflector was estimated as described in Chapter III. The mapping of the reflector is not free of errors. A standard deviation of 0.25 m was used for the position of the known reflector. This value was chosen to agree with the observations of [21].

1. Single Source-single Reflectors

In the first scenario, a single reflector provides strong multipath components and a single transmitting source with position $\left(x_S, y_S\right) = \left(170\text{ m}, 230\text{ m}\right)$ exists in the field. The

reflector has orientation $\theta_1 = 10^o$ with respect to the x-axis. The reference point of the reflector is y_R, located at $(0, 400\text{ m})$. The WSN covers a square area of $45\text{ m} \times 45\text{ m}$ centered at the origin. The general layout of scenario 1 is shown in Figure 29. Seventy five Monte Carlo simulations were conducted and a comparison was made between the proposed scheme which exploits the NLOS signals and the LOS-only-based scheme. Each array was comprised of 50 sensor elements randomly distributed in an area of 225 m^2.

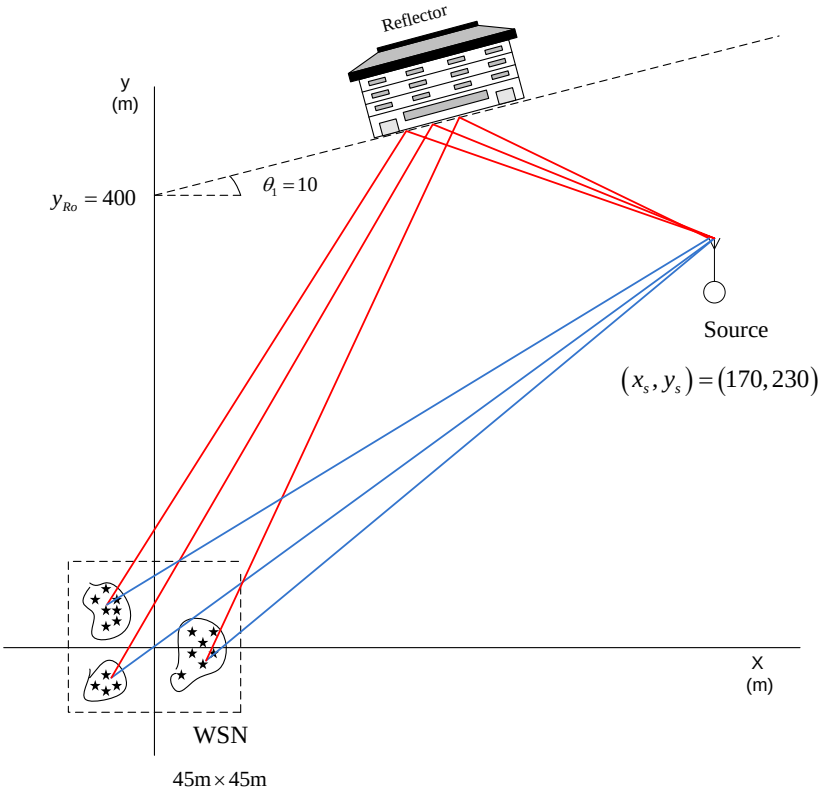

Figure 29. Scenario 1: Single source located at $(170\text{ m}, 230\text{ m})$. Single reflector with orientation $\theta_1 = 10^o$ and reference point at $y_{R1} = 400\text{ m}$. Variable number of arrays randomly distributed in a 2025 m^2 area.

The proposed localization scheme outperforms the LOS-only based localization as shown in Figure 30. This is because more bearings are available to the proposed scheme to formulate the position estimate. Additionally, the condition number of matrix A was found to be smaller for the proposed scheme as shown in Table 4. The signals

from a common source (i.e., actual source or reflector) will tend to be clustered in a realistic wireless sensor network scenario since the relative distance to the source of interest is typically large when compared with the spacing between neighboring arrays. However, the angle separation between those clusters is also relatively large. This is why the least squares problem for the proposed scheme is well conditioned compared with the LOS-only localization scheme

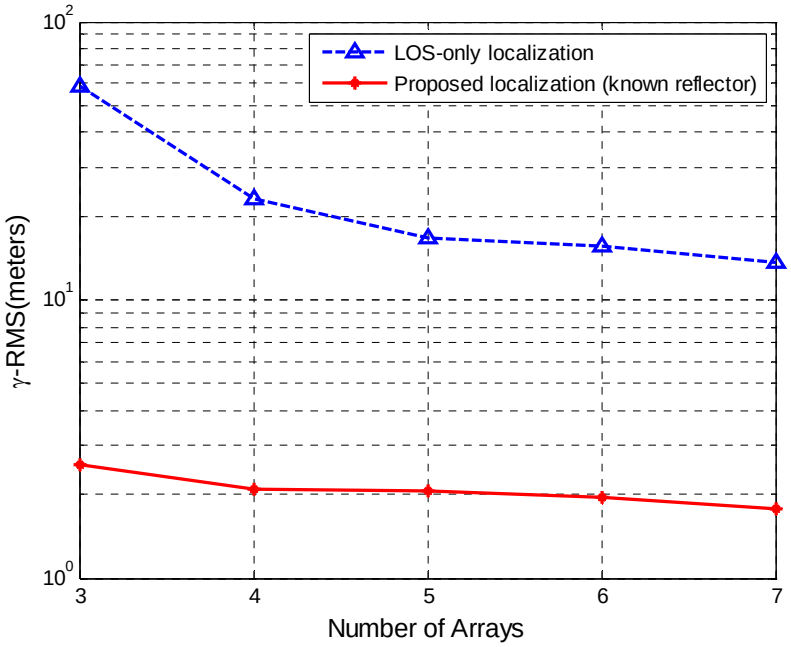

Figure 30. Scenario 1: RMS error for both the proposed scheme (LOS and NLOS signals) and the LOS-only based localization scheme in the presence of known reflectors.

Array	3	4	5	6	7
$k(A_1)$	57.8158	30.3956	26.7982	25.3431	24.4903
$k(A_2)$	2.5343	2.543	1.7376	1.6736	1.7588

Table 4. Scenario 1: Condition numbers as a function of the number of arrays for the LOS-only localization (A_1) and the proposed localization scheme (A_2), respectively.

The effect of the conditioning of the least squares problem for both the LOS-only and the proposed LOS-NLOS localization schemes is shown in Figure 31 where the RMS error is presented as a function of the distance between the source and the WSN. Three arrays of 30 sensors each were used. The proposed LOS-NLOS scheme provides accurate source position estimates when the distance is large while the LOS-only scheme is numerically unstable and inaccurate. We found that in many of the Monte Carlo simulations the LS problem of the LOS-only scheme is ill conditioned for source-array distances larger than 600 meters.

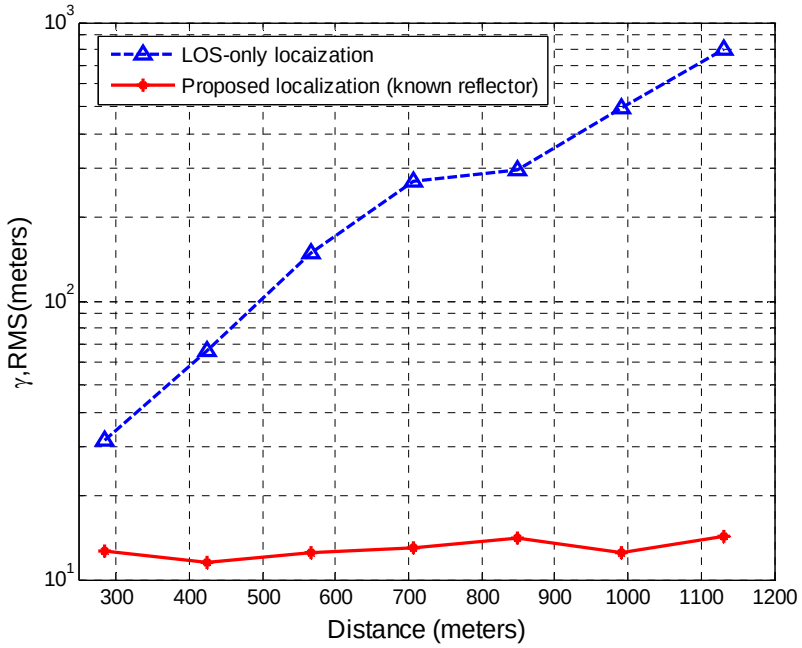

Figure 31. Scenario 1: RMS error as a function of the distance of the source from the arrays for both the proposed scheme (LOS and NLOS signals) and the LOS-only based localization scheme in the presence of known reflectors

A comparison between the centralized and the distributed localization scheme is shown in Figure 32. Both implementations perform similarly well, but in this particular example, the distributed approach is seen to be slightly more accurate. Additionally, for the reasons discussed earlier, the distributed approach is the more suitable approach for a WSN.

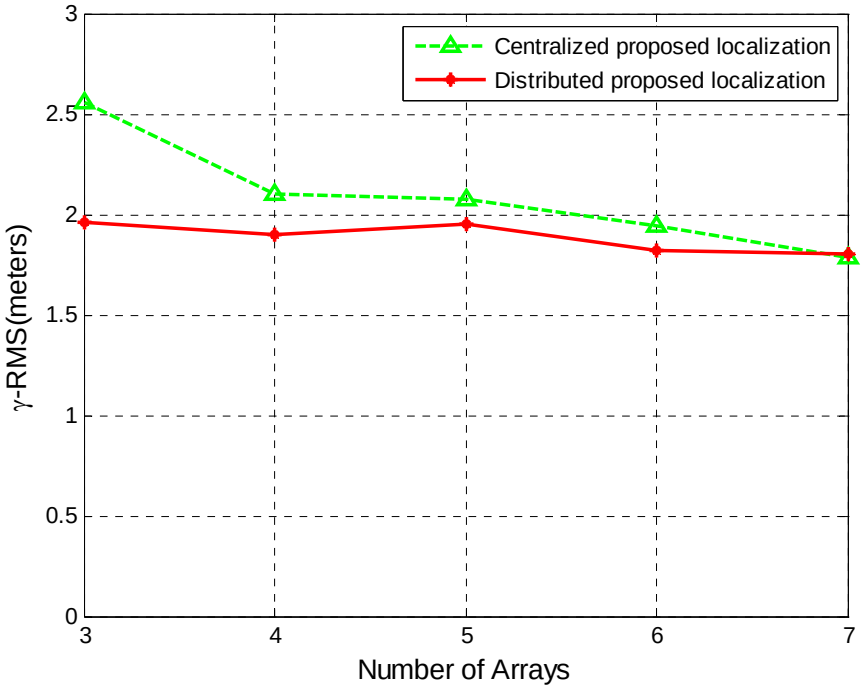

Figure 32. Scenario 1: RMS error for both the centralized and the distributed configuration of the proposed

The accuracy of the proposed localization scheme is reduced when the reflector position and orientation is unknown. Figure 33. compares the accuracy of the proposed scheme for both known and unknown reflectors with the LOS-only based localization scheme. An iterative approach, which updates the estimated reflector position, improves the accuracy of the proposed scheme. Figure 34 presents this improvement for the proposed localization scheme as a function of the number of iterations when the sequential LS approach is used for five arrays.

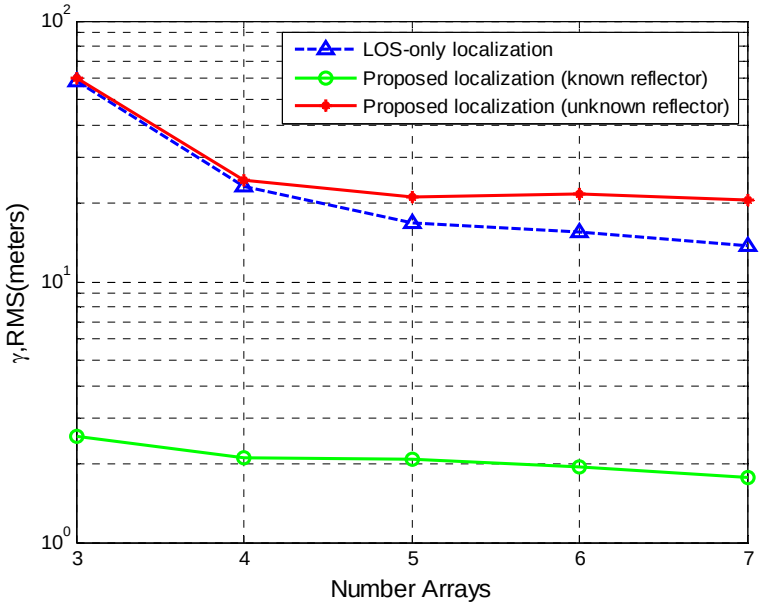

Figure 33. Scenario 1: RMS error for the proposed localization scheme using known and unknown reflectors and the LOS-only based localization scheme.

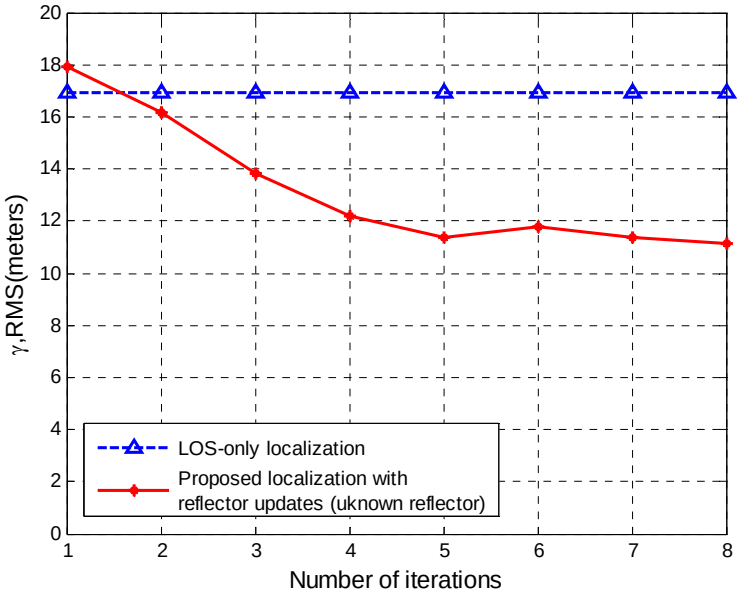

Figure 34. Scenario 1: RMS error as a function of the number of iterations for the proposed localization scheme with an unknown reflector using the sequential LS approach with five arrays.

As discussed earlier, matrix A of the least squares problem includes errors. Thus, the proposed localization scheme was also implemented using the TLS solution. This TLS solution outperforms the LS solution as shown in Figure 35. This is in contrast with what was found for the LOS–only based localization scheme in Chapter III and is the result of the well-conditioned nature of the proposed scheme. However, the improved location accuracy is achieved at the expense of the larger processing load required by the singular value decomposition which makes it difficult to deploy in a WSN.

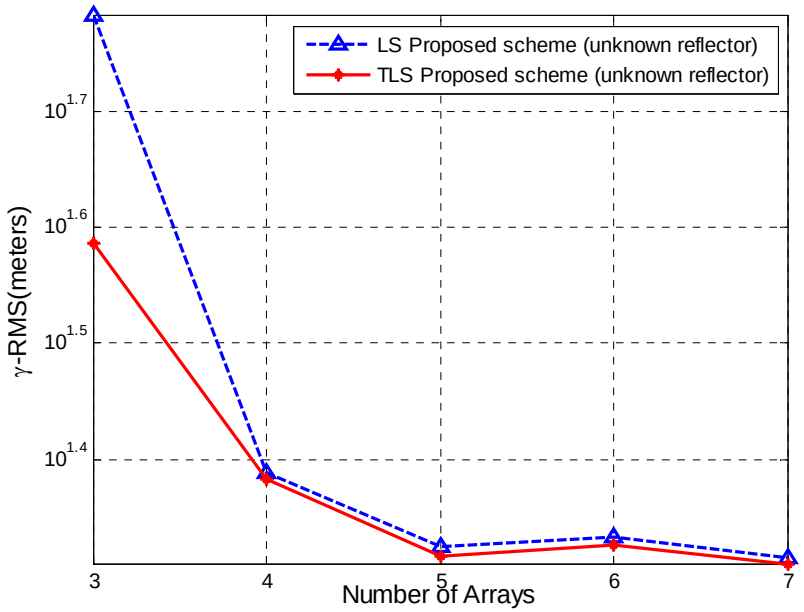

Figure 35. Scenario 1: RMS error for the proposed localization scheme using least squares solution and the total least squares solution.

2. Single Source-multiple Reflectors

The second scenario examines the accuracy of the proposed scheme when two reflectors are present. The geometric configuration is shown in Figure 36 and is the same as in scenario 1, except that an additional reflector exists with orientation $\theta_2 = 10^o$ and at reference point $y_{R_2} = -300$ m . Again 75 Monte Carlo simulations were conducted and a comparison was made between the proposed scheme which exploits the NLOS signals and the LOS-only-based scheme. Each array was comprised of 50 sensor elements randomly distributed in an area of $225\ \text{m}^2$.

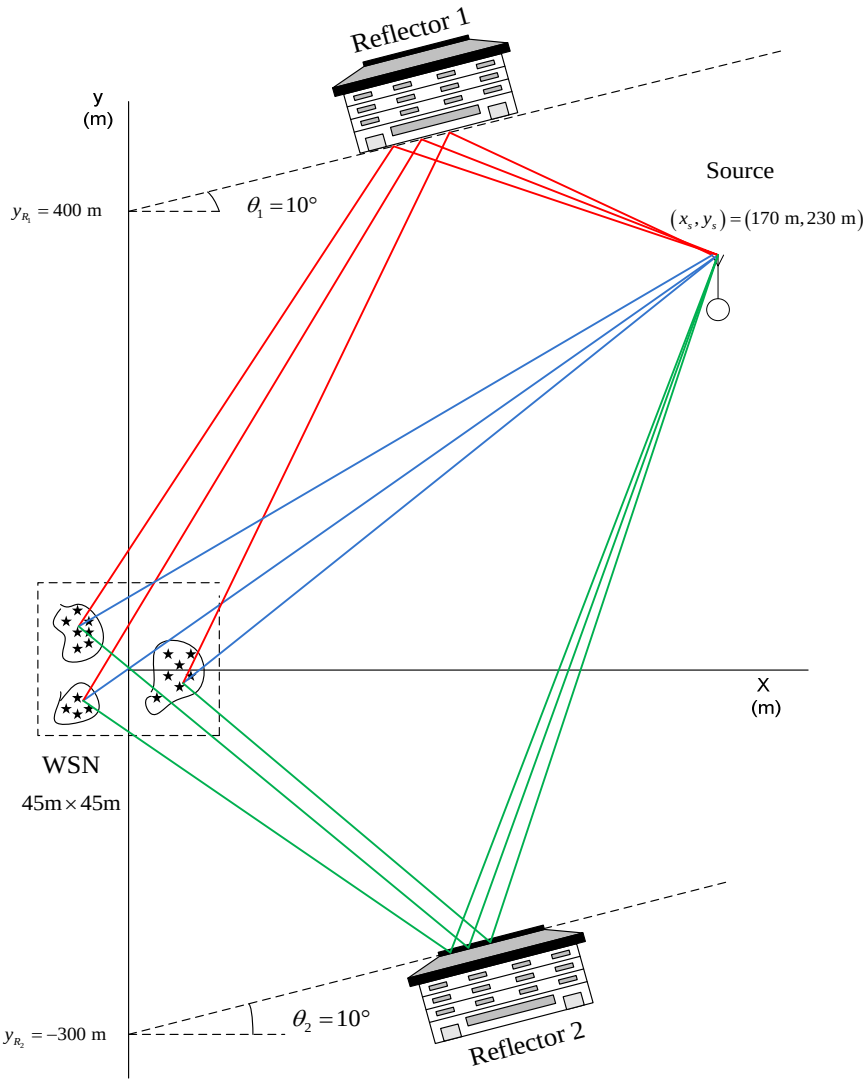

Figure 36. Scenario 2: Single source located at $(170\text{ m}, 230\text{ m})$. Two reflectors, both with orientation $\theta = 10^o$ and reference point at $y_{R1} = 400$ m and $y_{R2} = -300$ m respectively. A variable number of arrays were randomly distributed in a 2025 m^2 square area.

The proposed localization scheme outperforms the LOS-only based localization as shown in Figure 37 when the reflectors are known. Furthermore, when analyzing a LOS-based scheme, one must consider the case in which the scheme incorrectly identifies a NLOS signal to be LOS. As shown in Figure 38, this misidentification causes the LOS-only approach to completely break down and return erroneous results. In contrast, the proposed scheme, by design, effectively associates the incoming signals.

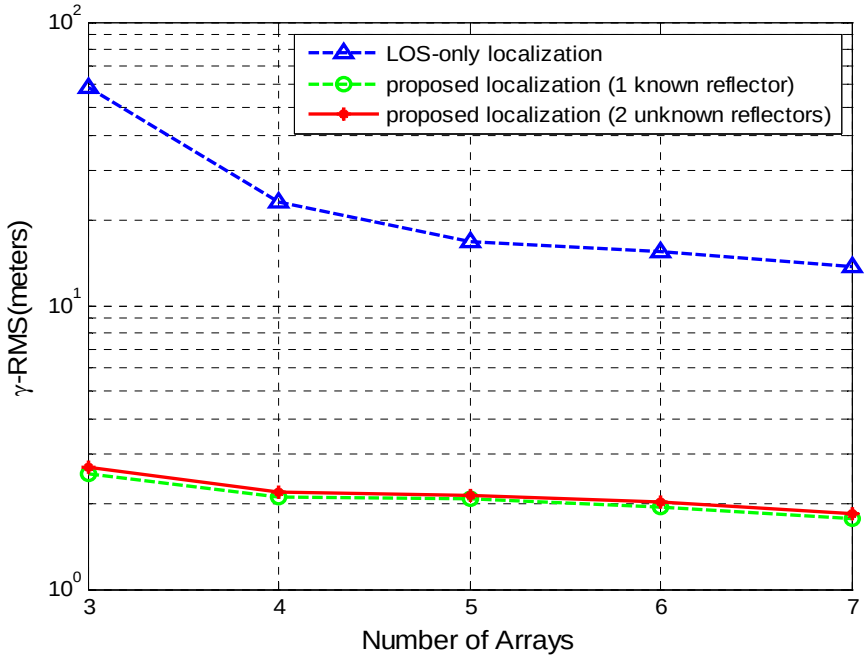

Figure 37. Scenario 2: RMS error for both the proposed scheme (LOS and NLOS signals) and the LOS-only based localization scheme in the presence of one and two known reflectors

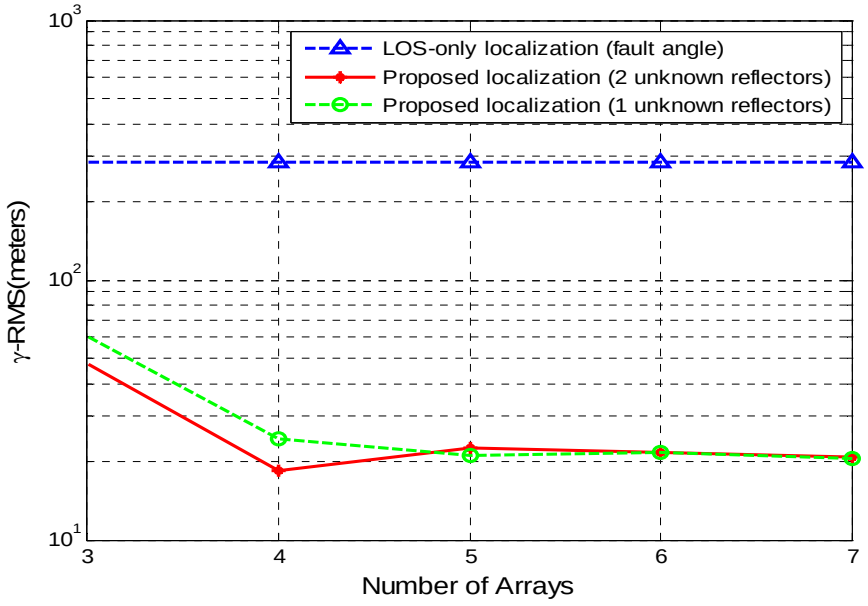

Figure 38. Scenario 2: RMS error for both the proposed scheme (LOS and NLOS signals) and the LOS-only based localization scheme when the latter takes one NLOS signal as the LOS signal.

The proposed localization scheme can also be used for NLOS-only localization. As shown in Figure 39, these estimates are significantly improved when more than one reflector is present (as is typically the case in a realistic scenario). This is also due to the clustered nature of the bearings, as discussed earlier, which affect the conditioning of the least squares problem. The condition numbers of the A matrix as a function of the number of arrays for NLOS-only localization in the presence of one and 2 reflectors are shown in Table 5.

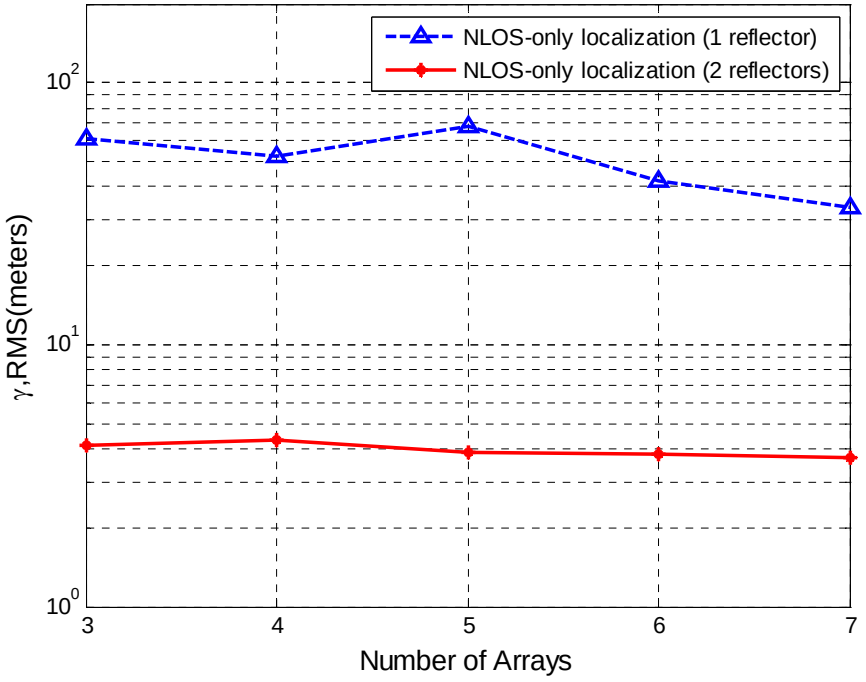

Figure 39. Scenario 2: RMS error for the NLOS-only localization of the proposed localization scheme in the presence of one and two known reflectors.

Array	3	4	5	6	7
$k(A_3)$	147.7123	98.8117	84.1275	76.5002	75.3193
$k(A_4)$	3.7182	3.7283	3.7319	3.7366	3.7435

Table 5. Condition numbers as a function of the number of arrays for the NLOS-only localization of the proposed localization scheme in the presence of one reflector (A_1) and two reflectors (A_2), respectively.

C. SUMMARY

In this chapter, simulation results were provided to validate the performance of the proposed localization scheme. We began with a discussion of the MATLAB simulation code and the performance metrics. Following this, simulation results were provided and analyzed for both the single reflector and the multiple reflector cases.

THIS PAGE INTENTIONALLY LEFT BLANK

V. CONCLUSION

This thesis proposed a least squares error estimator. Based on the proposed estimator, this thesis developed a passive source localization scheme which exploits the NLOS signals from non-cooperative sources. The proposed solution is a hybrid DOA/TDOA source localization scheme and is comprised of three parts: a DOA estimator, an association algorithm for the identified signal bearings, and the source localization scheme itself. This scheme allows a wireless sensor network to (1) perform single array localization, (2) perform the localization in a distributed fashion, (3) obtain source location estimates with NLOS signals only and (4) improve the location estimates compared with those obtained using the LOS information only. The proposed solution requires the knowledge of the position of potential reflectors which can be obtained dynamically using the included reflector mapping algorithm. A reflector knowledge updating procedure based on the sequential least squares was used when the reflectors were unknown and the accuracy of the proposed scheme was further improved. Simulation results were provided to demonstrate the effectiveness of the proposed scheme and the conditioning of the least squares problem associated with it and compare it to existing solutions.

A. SIGNIFICANT CONTRIBUTIONS

There are two significant contributions in this thesis. The first is a least squares error estimator for DOA localization which is unbiased when the noise is Gaussian-distributed with zero mean. This estimator solves an over determined Vandermonde system of equations which is known to be computationally efficient and accurate.

The second significant contribution of this thesis is a passive source localization scheme which exploits the NLOS signals from non-cooperative sources. The simulation results showed that the proposed localization scheme provided high accuracy estimates and outperformed the LOS-only based localization schemes. This is because more bearings are available and the conditioning of the least squares problem is better for the proposed scheme

B. FUTURE WORK

Throughout this thesis, it has been assumed that the positions of the sensors are known without errors. The presence of errors affects the accuracy of the DOA estimations and in turn the accuracy of the proposed localization scheme. A future effort may examine methods to reduce the impact of those errors.

This thesis did not address initial signal of interest (SOI) detection. Since the SOI SNR at the receiving sensor network is dependent to a large degree on the characteristics of the non-cooperative emitter, future work could include a study of SOI detection, and subsequent localization, as a function of received SNR.

This thesis assumed stationary sources and arrays. This assumption can be extended to include platforms that are moving at low speeds. A future effort could also examine the performance of the proposed scheme in tracking applications.

A signal power threshold was used to ensure that all reflections are “single bounce.” Future work may solve the association problem of multiple-hop reflections and exploit the information contained in those reflections.

Finally, an analysis which compares the computational cost of both the centralized and the distributed configurations of the proposed localization scheme may be a subject for a future work.

APPENDIX

This is the Matlab code used in this thesis to evaluate the performance of the proposed source localization scheme in the presence of one or two reflectors.

```
%THESIS MATLAB CODE
%Created by Georgios Tsivgoulis


clear; clc; clf reset;

%% TRANSMITTED SIGNAL

f=3E8;                                  % freq of baseband modulation
TB=1/(4*f);                             % time bandwidth product = 4
Nchips=64;                              % Number of Chips / Time seq
SPC = 16;                               % Samples Per Chip
cp=3E8;                                 % speed of light
lambda = cp/f;                          % c/f
k = 2*pi/lambda;                        % wavenumber
tend=SPC*Nchips;                        % time snapshot end
t=[0:(tend-1)]*TB/(tend-1);             % discritization of signal
s=sin(2*pi*f*t);
S=zeros(1,length(t));                   %incident signal
S(1,:) =S(1,:)+exp(1j*(s));

%Signal SNR
P=10^-4;                                % signal power (watt)
K=1.38*10^-23;                          % Boltzman constant
Tk=400;                                 % system temperature
B=3E4;                                  % signal bandwidth
SNR=10*log10(P/(K*Tk*B))                % signal SNR

%% TARGET POSITION-REFLECTOR SIMULATION

%%%%%%%%%%%%%%%%%%%%%%%%%%%%%%%%%%%%%%%%%%%%%%%%
%Simulation of the source and the arrays
%%%%%%%%%%%%%%%%%%%%%%%%%%%%%%%%%%%%%%%%%%%%%%%%

tic
Xt=170; Yt=230;                          % targets position
stdev=0.25;                              % reflector position
deviation
T=[Xt Yt];
Rt=sqrt(T(1)^2+T(2)^2);                  % source distance
tho1=10*pi/180;                          % reflector 1 orientation
YRo1=400;                                % reflector 1 reference point
tho2=-5*pi/180;                          % reflector 2 orientation
YRo2=-300;                               % reflector 2 reference point
```

```
c=input('give the number of clusters-receivers:')
array_size=input('give the size of the array:')
N=input('give the number of sensors/cluster:')
nruns=input('give the number of Monte carlo estimates:')
% array position
 Xs=zeros(1,c);Ys=zeros(1,c);
%for i=1:(c-1)/2;
%Ys(2*i)=15*i;
%Xs(2*i+1)=15*i;
%end

for run=1:nruns;              % Monte carlo simulation begin  from here
    fprintf('run:%2.0f\n',run);
   YRo1=YRo1+stdev*randn;
    YRo2=YRo2+stdev*randn;
for i=1:c;
    Ys(i)=45*rand;
    Xs(i)=45*rand;
tan_thL=(Yt-Ys(i))/(Xt-Xs(i));
thL=atan(tan_thL);

%%%%%%%%%%%%%%%%%%%%%%%%%%%%%%
%Simulation of the reflector
%%%%%%%%%%%%%%%%%%%%%%%%%%%%%%

%REFLECTOR1
XRs1=(1/(1+tan(tho1)^2))*Xs(i)+(tan(tho1)/(1+tan(tho1)^2))*(Ys(i)-
YRo1);
YRs1=tan(tho1)*XRs1+YRo1;
Xsim1=2*XRs1-Xs(i);
Ysim1=2*YRs1-Ys(i);
thA1=2*tho1+atan((Ysim1-T(2))/(T(1)-Xsim1)); %DOA  REF actual #1
XR11=50; YR11=tan(tho1)*XR11+YRo1;
XR12=200; YR12=tan(tho1)*XR12+YRo1;
th11=atan((YR11-Ys(i))/(XR11-Xs(i)))+5*pi/180;
th12=atan((YR12-Ys(i))/(XR12-Xs(i)))-3*pi/180;

%REFLECTOR2
XRs2=(1/(1+tan(tho2)^2))*Xs(i)+(tan(tho2)/(1+tan(tho2)^2))*(Ys(i)-
YRo2);
YRs2=tan(tho2)*XRs2+YRo2;
Xsim2=2*XRs2-Xs(i);
Ysim2=2*YRs2-Ys(i);
thA2=2*tho2+atan((Ysim2-T(2))/(T(1)-Xsim2)); %DOA  REF actual #2
XR21=50; YR21=tan(tho2)*XR21+YRo2;
XR22=200; YR22=tan(tho2)*XR22+YRo2;
th21=atan((YR21-Ys(i))/(XR21-Xs(i)))-5*pi/180;
th22=atan((YR22-Ys(i))/(XR22-Xs(i)))+3*pi/180;

%% RECEIVED SIGNAL

%%%%%%%%%%%%%%%%%%%%%%%%%%%%%%
%Signal strength simulation
%%%%%%%%%%%%%%%%%%%%%%%%%%%%%%
```

```
%Array Gain
GA=10*log10(N)+2;                %Assume dipole antenna elements

%Free space path loss
dL=sqrt((Xt-Xs(i))^2+(Yt-Ys(i))^2);
LSL=-20*log10(lambda)+20*log10(dL)+21.98;
dA1=sqrt((Xt-Xsim1)^2+(Yt-Ysim1)^2);
LSA1=-20*log10(lambda)+20*log10(dA1)+21.98;
dA2=sqrt((Xt-Xsim2)^2+(Yt-Ysim2)^2);
LSA2=-20*log10(lambda)+20*log10(dA2)+21.98;

%Reflection loss
thT1=asin(sin(pi/2-thA1)/sqrt(5));
Href1=(cos(pi/2-thA1)-sqrt(5)*cos(thT1))/(cos(pi/2-
thA1)+sqrt(5)*cos(thT1));
Lref1=20*log10(abs(Href1));

thT2=asin(sin(pi/2+thA2)/sqrt(5));
Href2=(cos(pi/2+thA2)-
sqrt(5)*cos(thT2))/(cos(pi/2+thA2)+sqrt(5)*cos(thT2));
Lref2=20*log10(abs(Href2));

%Received SNR
SNRL=SNR-LSL+GA;
SNRA1=SNR-LSA1+Lref1+GA;
SNRA2=SNR-LSA2+Lref2+GA;

%%%%%%%%%%%%%%%%%%%%%%%%%%%%%%%%%%
%Received Signal simulation
%%%%%%%%%%%%%%%%%%%%%%%%%%%%%%%%%%

[B1,B2,B3,B] =resignal(thL,thA1,thA2,N,array_size,k);
XL=B1*S; %Received signal
XL=awgn(XL,SNRL,'measured');
XA1=B2*S; %Received signal
XA1=awgn(XA1,SNRA1,'measured');
XA2=B3*S; %Received signal
XA2=awgn(XA2,SNRA2,'measured');
X=XA1+XA2+XL;

%% DOA ESTIMATION
thESTsdma=doa_sdma(X,B,N);
%thESTsdma2=doa_sdma(XA1,B,N);
%thESTsdma3=doa_sdma(XA2,B,N);
%thESTsdma=[thESTsdma1;thESTsdma2;thESTsdma3];

%% BEARING ASSOCIATION
%LOS=find(thESTsdma>th11 | thESTsdma<th12 |thESTsdma>th21 |
thESTsdma>th22 );
REF1=find(thESTsdma<th11 & thESTsdma>th12);
REF2=find(thESTsdma>th21 & thESTsdma<th22);
LOS=find(thESTsdma<th12&thESTsdma>th22);
thLest(i)=thESTsdma(LOS);
```

```
thAest1(i)=thESTsdma(REF1);
thAest2(i)=thESTsdma(REF2);
end

%% LOCALIZATION

%%%%%%%%%%%%%%%%%%%
%Matrix Formulation
%%%%%%%%%%%%%%%%%%%
for j=3:c;
    for i=1:j
A(i,:)=[1 -tan(thLest(i))];
A(i+j,:)=[1 -tan(2*tho1-thAest1(i))];
A(i+2*j,:)=[1 -tan(2*tho2-thAest2(i))];
b(i,1)=Ys(i)-tan(thLest(i))*Xs(i);
b(i+j,1)= Ysim1-tan(2*tho1-thAest1(i))*Xsim1;
b(i+2*j,1)= Ysim2-tan(2*tho2-thAest2(i))*Xsim2;

%Matrix formulation for image pointS
Aref1(i,:)=[1 -tan(thAest1(i))];
bref1(i,1)=Ys(i)-tan(thAest1(i))*Xs(i);
Aref2(i,:)=[1 -tan(thAest2(i))];
bref2(i,1)=Ys(i)-tan(thAest2(i))*Xs(i);
    end


%%%%%%%%%%%%%%%%%%%%%%%%%%%%%%%%%%%%
%1)LOS-only localization
%%%%%%%%%%%%%%%%%%%%%%%%%%%%%%%%%%%%

Xest1 =A(1:j,:)\b(1:j,1)
Rtest1=sqrt(Xest1(1)^2+Xest1(2)^2);
Y1=A(1:j,:)*Xest1;
kappa1=cond(A(1:j,:));
theta1=asin(norm(b(1:j,1)-Y1)/norm(b(1:j,1)));
eta1=norm(A(1:j,:))*norm(Xest1)/norm(Y1);

Condbx1(run,j-2)=kappa1/(eta1*cos(theta1));
CondAx1(run,j-2)=kappa1+(kappa1^2*tan(theta1))/eta1;
Yt_sdma1(run,j-2)=Xest1(1);
Xt_sdma1(run,j-2)=Xest1(2);

%Bias of the Target location
biasYt_sdma1(run,j-2)=T(2)-Xest1(1);
biasXt_sdma1(run,j-2)=T(1)-Xest1(2);
biasRt_sdma1(run,j-2)=Rt-Rtest1;

 %REFLECTOR DETERMINATION%
 %REFLECTOR1
Xestref1 =Aref1(1:j,:)\bref1(1:j,1);

tan_thM1=(Xestref1(1)-Xest1(1))/(Xest1(2)-Xestref1(2));
tho_est1=((pi/2)-atan(tan_thM1));
```

```
tho_est1*180/pi;
YRo_est1=(Xest1(1)+Xestref1(1))/2-
tan(tho_est1)*((Xest1(2)+Xestref1(2))/2);
 Xestref2 =Aref2\bref2;
%REFLECTOR2
tan_thM2=(Xestref2(1)-Xest1(1))/(Xest1(2)-Xestref2(2));
tho_est2=((pi/2)-atan(tan_thM2));
tho_est2*180/pi;
YRo_est2=(Xest1(1)+Xestref2(1))/2-
tan(tho_est2)*((Xest1(2)+Xestref2(2))/2);



XRsest1=(1/(1+tan(tho_est1)^2))*Xs(i)+(tan(tho_est1)/(1+tan(tho_est1)^2
))*(Ys(i)-YRo_est1);
YRsest1=tan(tho_est1)*XRsest1+YRo_est1;
Xsimest1=2*XRsest1-Xs(i);
Ysimest1=2*YRsest1-Ys(i);

XRsest2=(1/(1+tan(tho_est2)^2))*Xs(i)+(tan(tho_est2)/(1+tan(tho_est2)^2
))*(Ys(i)-YRo_est2);
YRsest2=tan(tho_est2)*XRsest2+YRo_est2;
Xsimest2=2*XRsest2-Xs(i);
Ysimest2=2*YRsest2-Ys(i);

%Matrix Formulation
for i=1:j
Ar(i,:)=[1 -tan(thLest(i))];
Ar(i+j,:)=[1 -tan(2*tho_est1-thAest1(i))];
Ar(i+2*j,:)=[1 -tan(2*tho_est2-thAest2(i))];
br(i,1)=Ys(i)-tan(thLest(i))*Xs(i);
br(i+j,1)= Ysimest1-tan(2*tho_est1-thAest1(i))*Xsimest1;
br(i+2*j,1)= Ysimest2-tan(2*tho_est2-thAest2(i))*Xsimest2;
end

%%%%%%%%%%
%%%%%%%%%%
%SCENARIO 1
%%%%%%%%%%
%%%%%%%%%%

%%%%%%%%%%%%%%%%%%%%%%%%%%%%%%%%%%%%%%%%%%%%%%%%%%%%%%%%%%%%%%%%%%%%%%%%
%2)Scenario 1:Centralized proposed localization(1 known reflector)
%%%%%%%%%%%%%%%%%%%%%%%%%%%%%%%%%%%%%%%%%%%%%%%%%%%%%%%%%%%%%%%%%%%%%%%%

A2=A(1:2*j,:); b2=b(1:2*j,:);
Xest2=A2\b2
 Y2=A2*Xest2;
Rtest2=sqrt(Xest2(1)^2+Xest2(2)^2);
Yt_sdma2(run,j-2)=Xest2(1);
Xt_sdma2(run,j-2)=Xest2(2);

kappa2=cond(A2);
theta2=asin(norm(b2-Y2)/norm(b2));
```

```
eta2=norm(A2)*norm(Xest2)/norm(Y2);
Condbx2(run,j-2)=kappa2/(eta2*cos(theta2));
CondAx2(run,j-2)=kappa2+(kappa2^2*tan(theta2))/eta2;

%Bias of the Target location
biasYt_sdma2(run,j-2)=T(2)-Xest2(1);
biasXt_sdma2(run,j-2)=T(1)-Xest2(2);
biasRt_sdma2(run,j-2)=Rt-Rtest2;

%%%%%%%%%%%%%%%%%%%%%%%%%%%%%%%%%%%%%%%%%%%%%%%%%%%%%%%%%%%%%%%%%%%%%%%%%%%%
%3)Scenario 1:Distributed propossed localization (1 known reflector)
%%%%%%%%%%%%%%%%%%%%%%%%%%%%%%%%%%%%%%%%%%%%%%%%%%%%%%%%%%%%%%%%%%%%%%%%%%%%
for i=1:j
A3=[A(i,:);A(i+j,:)];
b3=[b(i);b(i+j)];
Test3(:,i)=A3\b3;
end
Xest3=mean(Test3,2);
Yt_sdma3(run,j-2)=Xest3(1);
Xt_sdma3(run,j-2)=Xest3(2);
Rtest3=sqrt(Xest3(1)^2+Xest3(2)^2);
%Bias of the Target location
biasYt_sdma3(run,j-2)=T(2)-Xest3(1);
biasXt_sdma3(run,j-2)=T(1)-Xest3(2);
biasRt_sdma3(run,j-2)=Rt-Rtest3;

%%%%%%%%%%%%%%%%%%%%%%%%%%%%%%%%%%%%%%%%%%%%%%%%%%%%%%%%%%%%%%%%%%%%%%%%%%%%
%4)Scenario 1:Centralized proposed localization (1 unknown reflector)
%%%%%%%%%%%%%%%%%%%%%%%%%%%%%%%%%%%%%%%%%%%%%%%%%%%%%%%%%%%%%%%%%%%%%%%%%%%%
A4=Ar(1:2*j,:);
b4=br(1:2*j,:);

Xest4 =A4\b4; Y4=A4*Xest4;
Rtest4=sqrt(Xest4(1)^2+Xest4(2)^2);
Yt_sdma4(run,j-2)=Xest4(1);
Xt_sdma4(run,j-2)=Xest4(2);


%Bias of the Target location
biasYt_sdma4(run,j-2)=T(2)-Xest4(1);
biasXt_sdma4(run,j-2)=T(1)-Xest4(2);
biasRt_sdma4(run,j-2)=Rt-Rtest4;

%%%%%%%%%%%%%%%%%%%%%%%%%%%%%%%%%%%%%%%%%%%%%%%%%%%%%%%%%%%%%%%%%%%%%%%%%%%%
%5)Scenario 1:NLOS-only localization (1 known reflector)
%%%%%%%%%%%%%%%%%%%%%%%%%%%%%%%%%%%%%%%%%%%%%%%%%%%%%%%%%%%%%%%%%%%%%%%%%%%%
A5=A(j+1:2*j,:);
b5=b(j+1:2*j,1);
Xest5 =A5\b5;
Rtest5=sqrt(Xest5(1)^2+Xest5(2)^2);
Y5=A5*Xest5;
kappa5=cond(A5);
theta5=asin(norm(b5-Y5)/norm(b5));
eta5=norm(A5)*norm(Xest5)/norm(Y5);
```

```
Condbx5(run,j-2)=kappa5/(eta5*cos(theta5));
CondAx5(run,j-2)=kappa5+(kappa5^2*tan(theta5))/eta5;
Yt_sdma5(run,j-2)=Xest5(1);
Xt_sdma5(run,j-2)=Xest5(2);

%Bias of the Target location
biasYt_sdma5(run,j-2)=T(2)-Xest5(1);
biasXt_sdma5(run,j-2)=T(1)-Xest5(2);
biasRt_sdma5(run,j-2)=Rt-Rtest5;

%%%%%%%%%%%%%%%%%%%%%%%%%%%%%%%%%%%%%%%%%%%%%%%%%%%%%%%%%%%%%%%%%%%%%%%%%%%
%6)Scenario 1:Centrilized proposed localization (TLS, 1 reflector)
%%%%%%%%%%%%%%%%%%%%%%%%%%%%%%%%%%%%%%%%%%%%%%%%%%%%%%%%%%%%%%%%%%%%%%%%%%%
n1 = size(A4,2);
C = [A4 b4];
[U1 S1 V1] = svd(C,0);
V11 = V1(1:n1,1+n1:end);
V12 = V1(1+n1:end,1+n1:end);
Test6 = -V11/V12;
Rtest6=sqrt(Test6(1)^2+Test6(2)^2);

Yt_sdma6(run,j-2)=Test6(1);
Xt_sdma6(run,j-2)=Test6(2);

%Bias of the Target location
biasXt_sdma6(run,j-2)=T(2)-Test6(1);
biasYt_sdma6(run,j-2)=T(1)-Test6(2);
biasRt_sdma6(run,j-2)=Rt-Rtest6;


%%%%%%%%%%%%%%%%%%%%%%%%%%%%%%%%%%%%%%%%%%%%%%%%%%%%%%%%%%%%%%%%%%%%%%%%%%%
%7)Scenario2:Centralized proposed localization (2 known reflector)
%%%%%%%%%%%%%%%%%%%%%%%%%%%%%%%%%%%%%%%%%%%%%%%%%%%%%%%%%%%%%%%%%%%%%%%%%%%
Xest7=A\b
 Y7=A*Xest7;
Rtest7=sqrt(Xest7(1)^2+Xest7(2)^2);
Yt_sdma7(run,j-2)=Xest7(1);
Xt_sdma7(run,j-2)=Xest7(2);

kappa7=cond(A);
theta7=asin(norm(b-Y7)/norm(b));
eta7=norm(A)*norm(Xest7)/norm(Y7);
Condbx7(run,j-2)=kappa7/(eta7*cos(theta7));
CondAx7(run,j-2)=kappa7+(kappa7^2*tan(theta7))/eta7;

%Bias of the Target location
biasYt_sdma7(run,j-2)=T(2)-Xest7(1);
biasXt_sdma7(run,j-2)=T(1)-Xest7(2);
biasRt_sdma7(run,j-2)=Rt-Rtest7;

%%%%%%%%%%%%%%%%%%%%%%%%%%%%%%%%%%%%%%%%%%%%%%%%%%%%%%%%%%%%%%%%%%%%%%%%%%%
%8)Scenario 2:Centralized proposed localization (2 unknown reflector)
```

```
%%%%%%%%%%%%%%%%%%%%%%%%%%%%%%%%%%%%%%%%%%%%%%%%%%%%%%%%%%%%%%%%%%%%%%%%%%%%
Xest8 =Ar\br;
Rtest8=sqrt(Xest8(1)^2+Xest8(2)^2);
Yt_sdma8(run,j-2)=Xest8(1);
Xt_sdma8(run,j-2)=Xest8(2);


%Bias of the Target location
biasYt_sdma8(run,j-2)=T(2)-Xest8(1);
biasXt_sdma8(run,j-2)=T(1)-Xest8(2);
biasRt_sdma8(run,j-2)=Rt-Rtest8;

%%%%%%%%%%%%%%%%%%%%%%%%%%%%%%%%%%%%%%%%%%%%%%%%%%%%%%%%%%%%%%%%%%%%%%%%%%%%
%9)Scenario 2:Distributed proposed localization (2 known reflector)
%%%%%%%%%%%%%%%%%%%%%%%%%%%%%%%%%%%%%%%%%%%%%%%%%%%%%%%%%%%%%%%%%%%%%%%%%%%%
for i=1:j
A9=[A(i,:);A(i+j,:);A(i+2*j,:)];
b9=[b(i);b(i+j);b(i+2*j)];
Test9(:,i)=A9\b9;
end
Xest9=mean(Test9,2);
Yt_sdma9(run,j-2)=Xest9(1);
Xt_sdma9(run,j-2)=Xest9(2);
Rtest9=sqrt(Xest9(1)^2+Xest9(2)^2);
%Bias of the Target location
biasYt_sdma9(run,j-2)=T(2)-Xest9(1);
biasXt_sdma9(run,j-2)=T(1)-Xest9(2);
biasRt_sdma9(run,j-2)=Rt-Rtest9;

%%%%%%%%%%%%%%%%%%%%%%%%%%%%%%%%%%%%%%%%%%%%%%%%%%%%%%%%%%%%%%%%%%%%%%%%%%%%
%10)Scenario 2:NLOS-only (2 known reflector)
%%%%%%%%%%%%%%%%%%%%%%%%%%%%%%%%%%%%%%%%%%%%%%%%%%%%%%%%%%%%%%%%%%%%%%%%%%%%
A10=A(j+1:3*j,:);
b10=b(j+1:3*j,1);
Xest10 =A10\b10;
Rtest10=sqrt(Xest10(1)^2+Xest10(2)^2);
Y10=A10*Xest10;
kappa10=cond(A10);
theta10=asin(norm(b10-Y10)/norm(b10));
eta10=norm(A10)*norm(Xest10)/norm(Y10);

Condbx10(run,j-2)=kappa10/(eta10*cos(theta10));
CondAx10(run,j-2)=kappa10+(kappa10^2*tan(theta10))/eta10;
Yt_sdma10(run,j-2)=Xest10(1);
Xt_sdma10(run,j-2)=Xest10(2);

%Bias of the Target location
biasYt_sdma10(run,j-2)=T(2)-Xest10(1);
biasXt_sdma10(run,j-2)=T(1)-Xest10(2);
biasRt_sdma10(run,j-2)=Rt-Rtest10;

%%%%%%%%%%%%%%%%%%%%%%%%%%%%%%%%%%%%%%%%%%%%%%%%%%%%%%%%%%%%%%%%%%%%%%%%%%%%
%11)LOS-only localization (fault angle)
%%%%%%%%%%%%%%%%%%%%%%%%%%%%%%%%%%%%%%%%%%%%%%%%%%%%%%%%%%%%%%%%%%%%%%%%%%%%
```

```
for i=1:j-1;
A11(i+1,:)=[1 -tan(thLest(i+1))];
b11(i+1,:)=[1 -tan(thLest(i+1))];
end
A11(1,:)=[1 -tan(thAest1(1))];
b11(1,:)=[1 -tan(thAest1(1))];
Xest11 =A11\b11;
Rtest11=sqrt(Xest11(1)^2+Xest11(2)^2);
Yt_sdma11(run,j-2)=Xest11(1);
Xt_sdma11(run,j-2)=Xest11(2);

%Bias of the Target location
biasYt_sdma11(run,j-2)=T(2)-Xest11(1);
biasXt_sdma11(run,j-2)=T(1)-Xest11(2);
biasRt_sdma11(run,j-2)=Rt-Rtest11;

end
end

%% ERROR ANALYSIS

%1)Statistics for LOS-only localization
bias_sdma1=[biasXt_sdma1' biasYt_sdma1' biasRt_sdma1'];     %Matrix of
bias
meanbiasRt_sdma1=mean(biasRt_sdma1);                        %Mean
position error
varbiasRt_sdma1=var(biasRt_sdma1);                          %Variance
of position error
rmsbiasRt_sdma1=sqrt(meanbiasRt_sdma1.^2+varbiasRt_sdma1);  %RMS
position error

meanCondbx1=mean(Condbx1)
meanCondAx1=mean(CondAx1)

%2)Statistics for Centralized proposed localization(1 known reflector)
bias_sdma2=[biasXt_sdma2' biasYt_sdma2' biasRt_sdma2'];     %Matrix of
bias
meanbiasRt_sdma2=mean(biasRt_sdma2);                        %Mean
position error
varbiasRt_sdma2=var(biasRt_sdma2);                          %Variance
of position error
rmsbiasRt_sdma2=sqrt(meanbiasRt_sdma2.^2+varbiasRt_sdma2);  %RMS
position error

meanCondbx2=mean(Condbx2)
meanCondAx2=mean(CondAx2)


%3)Statistics for Distributed proposed localization(1 known reflector)
bias_sdma3=[biasXt_sdma3' biasYt_sdma3' biasRt_sdma3'];     %Matrix of
bias
meanbiasRt_sdma3=mean(biasRt_sdma3);                        %Mean
position error
```

```
varbiasRt_sdma3=var(biasRt_sdma3);                          %Variance
of position error
rmsbiasRt_sdma3=sqrt(meanbiasRt_sdma3.^2+varbiasRt_sdma3);  %RMS
position error

%4)Statistics for Centralized proposed localization(1 unknown
reflector)
bias_sdma4=[biasXt_sdma4' biasYt_sdma4' biasRt_sdma4'];     %Matrix of
bias
meanbiasRt_sdma4=mean(biasRt_sdma4);                        %Mean
position error
varbiasRt_sdma4=var(biasRt_sdma4);                          %Variance
of position error
rmsbiasRt_sdma4=sqrt(meanbiasRt_sdma4.^2+varbiasRt_sdma4);  %RMS
position error

%5)Statistics for NLOS-only localization (1 known reflector)
bias_sdma5=[biasXt_sdma5' biasYt_sdma5' biasRt_sdma5'];     %Matrix of
bias
meanbiasRt_sdma5=mean(biasRt_sdma5);                        %Mean
position error
varbiasRt_sdma5=var(biasRt_sdma5);                          %Variance
of position error
rmsbiasRt_sdma5=sqrt(meanbiasRt_sdma5.^2+varbiasRt_sdma5);  %RMS
position error

meanCondbx5=mean(Condbx5)
meanCondAx5=mean(CondAx5)

%6)Statistics for Centrilized proposed localization (TLS, 1 reflector)
bias_sdma6=[biasXt_sdma6' biasYt_sdma6' biasRt_sdma6'];     %Matrix of
bias
meanbiasRt_sdma6=mean(biasRt_sdma6);                        %Mean
position error
varbiasRt_sdma6=var(biasRt_sdma6);                          %Variance
of position error
rmsbiasRt_sdma6=sqrt(meanbiasRt_sdma6.^2+varbiasRt_sdma6);  %RMS
position error

%7)Statistics for Centralized proposed localization(2 known reflector)
bias_sdma7=[biasXt_sdma7' biasYt_sdma7' biasRt_sdma7'];     %Matrix of
bias
meanbiasRt_sdma7=mean(biasRt_sdma7);                        %Mean
position error
varbiasRt_sdma7=var(biasRt_sdma7);                          %Variance
of position error
rmsbiasRt_sdma7=sqrt(meanbiasRt_sdma7.^2+varbiasRt_sdma7);  %RMS
position error

meanCondbx7=mean(Condbx7)
meanCondAx7=mean(CondAx7)

%8)Statistics for Centralized proposed localization(2 known reflector)
```

```
bias_sdma8=[biasXt_sdma8' biasYt_sdma8' biasRt_sdma8'];     %Matrix of
bias
meanbiasRt_sdma8=mean(biasRt_sdma8);                        %Mean
position error
varbiasRt_sdma8=var(biasRt_sdma8);                          %Variance
of position error
rmsbiasRt_sdma8=sqrt(meanbiasRt_sdma8.^2+varbiasRt_sdma8);  %RMS
position error

%9)Statistics for Centralized proposed localization(2 unknown
reflector)
bias_sdma9=[biasXt_sdma9' biasYt_sdma9' biasRt_sdma9'];     %Matrix of
bias
meanbiasRt_sdma9=mean(biasRt_sdma9);                        %Mean
position error
varbiasRt_sdma9=var(biasRt_sdma9);                          %Variance
of position error
rmsbiasRt_sdma9=sqrt(meanbiasRt_sdma9.^2+varbiasRt_sdma9);  %RMS
position error

%10)Statistics for NLOS-only localization (1 known reflector)
bias_sdma10=[biasXt_sdma10' biasYt_sdma10' biasRt_sdma10'];  %Matrix of
bias
meanbiasRt_sdma10=mean(biasRt_sdma10);                       %Mean
position error
varbiasRt_sdma10=var(biasRt_sdma10);                         %Variance
of position error
rmsbiasRt_sdma10=sqrt(meanbiasRt_sdma10.^2+varbiasRt_sdma10);%RMS
position error

meanCondbx10=mean(Condbx10)
meanCondAx10=mean(CondAx10)

%11)Statistics for LOS-only localization (fault angle)
bias_sdma11=[biasXt_sdma11' biasYt_sdma11' biasRt_sdma11'];  %Matrix of
bias
meanbiasRt_sdma11=mean(biasRt_sdma11);                       %Mean
position error
varbiasRt_sdma11=var(biasRt_sdma11);                         %Variance
of position error
rmsbiasRt_sdma11=sqrt(meanbiasRt_sdma11.^2+varbiasRt_sdma11);%RMS
position error


toc

SN=3:7;

figure(1)
plot(SN,rmsbiasRt_sdma1,'b--^',SN,rmsbiasRt_sdma2,'r-*')
xlabel('Number Arrays','Fontsize',12)
ylabel('\gamma,RMS(meters)','Fontsize',12)
legend('LOS-only localization','Proposed localization (known
reflector)')
```

```
figure(2)
plot(SN,rmsbiasRt_sdma2,'g--^',SN,rmsbiasRt_sdma3,'r-*')
xlabel('Number of Arrays','Fontsize',12)
ylabel('\gamma-RMS(meters)','Fontsize',12)
legend('Centralized proposed localization','Distributed proposed
localization ')

figure(3)
plot(SN,rmsbiasRt_sdma1,'b-^',SN,rmsbiasRt_sdma2,'g-
o',SN,rmsbiasRt_sdma4,'r-*')
xlabel('Number of Arrays','Fontsize',12)
ylabel('\gamma,RMS(meters)','Fontsize',12)
legend('LOS-only localization','Proposed localization (known
reflector)',...
    'Proposed localization (unknown reflector)')

figure(4)
plot(SN,rmsbiasRt_sdma4,'r--^',SN,rmsbiasRt_sdma6,'r-*')
xlabel('Number of Arrays','Fontsize',12)
ylabel('\gamma,RMS(meters)','Fontsize',12)
legend('LS proposed scheme(unknown reflector)','TLS proposed
scheme(unknown reflector)')

figure(5)
plot(SN,rmsbiasRt_sdma1,'b--^',SN,rmsbiasRt_sdma2,'r-
*',SN,rmsbiasRt_sdma7,'r-*')
xlabel('Number Arrays','Fontsize',12)
ylabel('\gamma,RMS(meters)','Fontsize',12)
legend('LOS-only localization','Proposed localization (1 known
reflector)',...
    'Proposed localization (2 known reflector)')

figure(6)
plot(SN,rmsbiasRt_sdma11,'b--^',SN,rmsbiasRt_sdma8,'r-
*',SN,rmsbiasRt_sdma4,'g--o')
xlabel('Number of Arrays','Fontsize',12)
ylabel('\gamma,RMS(meters)','Fontsize',12)
legend('LOS-only localization (fault angle)','Proposed localization (1
unknown reflector)',...
    'Proposed localization (2 unknown reflector)')

figure(7)
plot(SN,rmsbiasRt_sdma5,'b--^',SN,rmsbiasRt_sdma10,'r-*')
xlabel('Number Arrays','Fontsize',12)
ylabel('\gamma,RMS(meters)','Fontsize',12)
legend('NLOS-only localization (1 reflector)','NLOS-only localization
(2 reflector)')
```

This is the Matlab code used in this thesis to evaluate the performance of the proposed source localization scheme in the presence one unknown reflector using the sequential least squares.

```
%MODEL WHICH APPLIES THE SEQUENTIAL LEAST SQUARE IN THE LOCALIZATION

clear; clc; clf reset;

Var=0.25*pi^2/180^2;
f=3E8;                                          % freq of baseband
modulation
TB=1/(4*f);                                      % time bandwidth product
= 4
Nchips=64;                                      % Number of Chips / Time
seq
SPC = 16;                                       % Samples Per Chip

cp=3E8;
lambda = cp/f;                                  % c/f
k = 2*pi/lambda;                                % wavenumber

tend=SPC*Nchips;                                % time snapshot end
t=[0:(tend-1)]*TB/(tend-1);                     % discritization of
signal
s=sin(2*pi*f*t);
S=zeros(1,length(t));                           %incident signal
S(1,:) =S(1,:)+exp(1j*(s));

%Signal Power
P=10^-4;
K=1.38*10^-23;
Tk=400;
B=3E4;
SNR=10*log10(P/(K*Tk*B))

%% TARGET POSITION-REFLECTOR SIMULATION
tic
Xt=170; Yt=230;                                                 % targets
position
stdev=0.25;
T=[Xt Yt];
Rt=sqrt(T(1)^2+T(2)^2);
tho1=10*pi/180;
YRo1=400;
c=input('give the number of clusters-receivers:')
array_size=input('give the size of the array:')
N=input('give the number of sensors/cluster:')
nruns=input('give the number of Monte carlo estimates:')
it=input('give the number of iterations')
Xs=zeros(1,c);Ys=zeros(1,c);
```

```
for run=1:nruns;                    % Monte carlo simulation begin  from
here
    fprintf('run:%2.0f\n',run);
   YRo1=YRo1+stdev*randn;
%Array positions
   for i=1:c;
    Ys(i)=45*rand;
    Xs(i)=45*rand;
tan_thL=(Yt-Ys(i))/(Xt-Xs(i));
thL=atan(tan_thL);

%%%%%%%%%%%%%%%%%%%%%%%%%%%%
%Simulation of the reflector
%%%%%%%%%%%%%%%%%%%%%%%%%%%%

XRs1=(1/(1+tan(tho1)^2))*Xs(i)+(tan(tho1)/(1+tan(tho1)^2))*(Ys(i)-
YRo1);
YRs1=tan(tho1)*XRs1+YRo1;
Xsim1=2*XRs1-Xs(i);
Ysim1=2*YRs1-Ys(i);
thA1=2*tho1+atan((Ysim1-T(2))/(T(1)-Xsim1)); %DOA  REF actual #1
XR11=50; YR11=tan(tho1)*XR11+YRo1;
XR12=200; YR12=tan(tho1)*XR12+YRo1;
th11=atan((YR11-Ys(i))/(XR11-Xs(i)))+5*pi/180;
th12=atan((YR12-Ys(i))/(XR12-Xs(i)))-3*pi/180;

%%%%%%%%%%%%%%%%%%%%%%%%%%%%
%Signal strength simulation
%%%%%%%%%%%%%%%%%%%%%%%%%%%%

%Array Gain
GA=10*log10(N)+2;               %Assume dipole antenna elements

%Free space path loss
dL=sqrt((Xt-Xs(i))^2+(Yt-Ys(i))^2);
LSL=-20*log10(lambda)+20*log10(dL)+21.98;
dA1=sqrt((Xt-Xsim1)^2+(Yt-Ysim1)^2);
LSA1=-20*log10(lambda)+20*log10(dA1)+21.98;

%Reflection loss
thT1=asin(sin(pi/2-thA1)/sqrt(5));
Href1=(cos(pi/2-thA1)-sqrt(5)*cos(thT1))/(cos(pi/2-
thA1)+sqrt(5)*cos(thT1));
Lref1=20*log10(abs(Href1));

%Received SNR
SNRL=SNR-LSL+GA;
SNRA1=SNR-LSA1+Lref1+GA;

%%%%%%%%%%%%%%%%%%%%%%%%%%%%%%%%%%
%Received Signal- DOA Estimation
%%%%%%%%%%%%%%%%%%%%%%%%%%%%%%%%%%
for j=1:it;
[B1,B2,B] =resignal(thL,thA1,N,array_size,k);
```

```
XL=B1*S; %Received signal
XL=awgn(XL,SNRL,'measured');
XA1=B2*S; %Received signal
XA1=awgn(XA1,SNRA1,'measured');
X=XA1+XL;
thESTsdma=doa_sdma(X,B,N);

%%%%%%%%%%%%%%%%%%%%%%%%
%Assosiation
%%%%%%%%%%%%%%%%%%%%%%%%
REF1=find(thESTsdma<th11 & thESTsdma>th12);
LOS=find(thESTsdma<th12);
thLest(i,j)=thESTsdma(LOS);
thAest1(i,j)=thESTsdma(REF1);
end
end
%%%%%%%%%%%%%%%%%%%
%Matrix Formulation for LOS and REF
%%%%%%%%%%%%%%%%%%%
for j=1:it;
for i=1:c;
Alos(i+c*j-c,:)=[1 -tan(thLest(i,j))];
blos(i+c*j-c,1)=Ys(i)-tan(thLest(i,j))*Xs(i);
Aref(i+c*j-c,:)=[1 -tan(thAest1(i,j))];
bref(i+c*j-c,1)=Ys(i)-tan(thAest1(i,j))*Xs(i);
end
end
Xestlos(:,1)=Alos(1:c,:)\blos(1:c,:);
Xestref(:,1)=Aref(1:c,:)\bref(1:c,:);

%%%%%%%%%%%%%%%%%%%%%%%%%%%%%%%%%%%%%%%%%%%%%%%%%%%%%%%%%%%%%%%%%%%%%%%%%%%%%%%
%Reflector estimation using sequential least square
%%%%%%%%%%%%%%%%%%%%%%%%%%%%%%%%%%%%%%%%%%%%%%%%%%%%%%%%%%%%%%%%%%%%%%%%%%%%%%%

for j=1:c*(it-1)
    C(1:j+c-1,1:j+c-1)=(1/Var)*eye(j+c-1);
    Sigmalos(:,:)=inv(Alos(1:j+c-1,:)'*C(1:j+c-1,1:j+c-1)*Alos(1:j+c-
1,:));
    Klos(:,j)=(Sigmalos(:,:)*Alos(j+c,:)')/(Var+Alos(j+c,:)*
Sigmalos(:,:)*Alos(j+c,:)');
Xestlos(:,j+1)=Xestlos(:,j)+Klos(:,j)*(blos(j+c,1)-
Alos(j+c,:)*Xestlos(:,j));

Sigmaref(:,:)=inv(Aref(1:j+c-1,:)'*C(1:j+c-1,1:j+c-1)*Aref(1:j+c-1,:));
    Kref(:,j)=(Sigmaref(:,:)*Aref(j+c,:)')/(Var+Aref(j+c,:)*
Sigmaref(:,:)*Aref(j+c,:)');
Xestref(:,j+1)=Xestref(:,j)+Kref(:,j)*(bref(j+c,1)-
Aref(j+c,:)*Xestref(:,j));
tan_thM=(Xestref(1,j)-Xestlos(1,j))/(Xestlos(2,j)-Xestref(2,j));
tho_est(j)=((pi/2)-atan(tan_thM));
YRo_est(j)=(Xestlos(1,j)+Xestref(1,j))/2-
tan(tho_est(j))*((Xestlos(2,j)+Xestref(2,j))/2);
for i=1:c;
XRsest(j,i)=(1/(1+tan(tho_est(j))^2))*Xs(i)+(tan(tho_est(j))/(1+tan(tho
_est(j))^2))*(Ys(i)-YRo_est(j));
```

```
YRsest(j,i)=tan(tho_est(j))*XRsest(j)+YRo_est(j);
Xsimest(j,i)=2*XRsest(j,i)-Xs(i);
Ysimest(j,i)=2*YRsest(j,i)-Ys(i);
Ar(i,:)=[1 -tan(thLest(i))];
Ar(i+c,:)=[1 -tan(2*tho_est(j)-thAest1(i))];
br(i,1)=Ys(i)-tan(thLest(i))*Xs(i);
br(i+c,1)= Ysimest(j,i)-tan(2*tho_est(j)-thAest1(i))*Xsimest(j,i);
end
Xest2=Ar\br
Rtest2=sqrt(Xest2(1)^2+Xest2(2)^2);
biasRt_sdma2(run,j)=Rt-Rtest2;
end

%Los localization
Xest1=Xestlos(:,1)
Rtest1=sqrt(Xest1(1)^2+Xest1(2)^2);
biasRt_sdma1(run)=Rt-Rtest1;
end

meanbiasRt_sdma1=mean(biasRt_sdma1);                          %Mean
position error
varbiasRt_sdma1=var(biasRt_sdma1);                            %Variance
of position error
rmsbiasRt_sdma1=sqrt(meanbiasRt_sdma1.^2+varbiasRt_sdma1);    %RMS
position error

meanbiasRt_sdma2=mean(biasRt_sdma2);                          %Mean
position error
varbiasRt_sdma2=var(biasRt_sdma2);                            %Variance
of position error
rmsbiasRt_sdma2=sqrt(meanbiasRt_sdma2.^2+varbiasRt_sdma2);    %RMS
position error

rmsbiasRt_sdma1=rmsbiasRt_sdma1*ones(1,8)
SN=1:8;
figure(1)
plot(SN,rmsbiasRt_sdma1,'b--^',SN,rmsbiasRt_sdma2,'r-*')
xlabel('Number of iterations','Fontsize',12)
ylabel('\gamma,RMS(meters)','Fontsize',12)
legend('LOS-only localization','LS proposed (known reflector)')
```

This is the function used to determine the received signal in the array

```
function [B1,B2,B] =resignal(thLOS,thREF1,N,array_size,k )


Ntheta=91; Nphi=3601;                        % Set up angle matrices
theta = linspace(0,pi/2,Ntheta);
phi   = linspace(-pi,pi,Nphi);
DTheta= theta(2)-theta(1); DPhi = phi(2)-phi(1);
[Phi,Theta] = meshgrid(phi,theta);
CT=cos(Theta); ST=sin(Theta); CP=cos(Phi); SP=sin(Phi);
Rx=ST.*CP; Ry=ST.*SP; Rz=CT;                 % unit radial vector
components


                                % in wavelengths (lambda) square grid
min_spacing =array_size/50 ;    % 1/10th wavelength
sepn_min = 0;                   % initialize prior to 1st test
xp = array_size * rand(1,N);
yp = array_size * rand(1,N);

%------------ Stats of Random Array ---------------

while (sepn_min< min_spacing)                % min spacing = .1
wavelength

    rp = [xp;yp]';
    sepn = pdist(rp);                        % dist between all
elements in Random Array
    sepn_min = min(sepn);                    % find minimum separation
    zsepn = squareform(sepn);                % convert linear sepn
array to square
    [Rmin Cmin] = find(zsepn==sepn_min,1, 'first'); %returns index
    if (sepn_min< min_spacing)               % then Move one of them
        xp(Rmin)=array_size * rand;
        yp(Rmin)=array_size * rand;
    end

m=find(theta==pi/2);                         % want row for xy plane
Rxm = Rx(m,:);                               % 1xNphi vector
Rym = Ry(m,:);

% Calculate the actual received signal for each angle using the N
element
% receiver and sum all N signals.
   for n=1:N
      B11(1,n) = exp(j*(k*(cos(thLOS)*xp(n)+sin(thLOS)*yp(n))));
     B22(1,n) =exp(j*(k*( cos(thREF1)*xp(n)+sin(thREF1)*yp(n))));
   end

for n=1:3601;
   an(n)=(n/10-0.1)-180;
```

```
   th(n)=an(n)*pi/180;
   for i=1:N
       B(i,n)=exp(1j*(k*(xp(i)*Rxm(n)+ yp(i)*Rym(n))));
   end
end
B1=B11';
B2=B22';
```

This is the function used to estimate the DOA of the incident signal using the SDMA receiver.

```
function thESTsdma=doa_sdma(X,B,N)

  %% SDMA RECEIVER

Nchips=64;
SPC = 16;                                % Samples Per Chip
H = hadamard(Nchips);                    % use Walsh Sequence
codes=[];
for i=1:N
    codes(i,:)=H(i+1,:);                 % don't want 1st row
end
% spread codes by SPC
codes = repmat( codes,SPC,1);            % repeat by spread factor
codes = reshape(codes,N,SPC*Nchips);     % move like chips together
codes = codes*pi/2;                      % pi/2 since inside exponential
codes=codes';
r=codes*X;

v=codes*B;
R=conj(v)'*r;
R=sum(R,2);
maxR=max(abs(R));
Psdma=abs(R)/maxR;
Psdma=[zeros(900,1); Psdma(902:2702,:); zeros(900,1)];

%DOA SDMA
Nphi=3601;
phi   = linspace(-pi,pi,Nphi);
for i=1:Nphi
if Psdma(i)>0.5;
    Psdma1(i)=Psdma(i);
else
    Psdma1(i)=0;
end
end

POSsdma = imregionalmax(Psdma1);              % MATLAB rtn that finds
local maxima->BW array "1"s
PEAKsdma = find(POSsdma);                     % index pointers to local
Maxima
```

```
[bs,is]=sort(Psdma(find(POSsdma)),'descend'); % sort by highest peak-
>lowest
ThESTsdma= PEAKsdma(is);                      % index to peaks
ThESTsdma= 180*phi(ThESTsdma)/pi;             % Angle where peaks occur
thESTsdma=ThESTsdma(1,1:2);
thESTsdma=thESTsdma*pi/180;
```

This is the function used to estimate the DOA of the incident signal using the MUSIC algorithm.

doa_music.m

```
function thESTmusic=doa_music(X,A,N)
Nchips=64;                          % Number of Chips / Time seq
SPC = 16;                           % Samples Per Chip
tend=SPC*Nchips;
Nphi=3601;
phi   = linspace(-pi,pi,Nphi);
Rxx=X*X'/tend;                      %autocorrelation matrix of signal
[V,Dia]=eig(Rxx);                   %eigenvalues of autocorrelation
matrix
[Y,Index]=sort(diag(Dia));          %eigenvalues in descending order
EN=V(:,Index(1:N-2));               %noise subspace matrix
for i=1:3601;
MU(i)=abs(A(:,i)'*EN*EN'*A(:,i));
end
Pmu=1./MU;                          %music pseudospectrum
maxPmu=max(Pmu);
Pmu=[Pmu(1802:3601) Pmu(1:1801)];
Pmusic=Pmu/maxPmu;
Pmusic=[zeros(1,900) Pmusic(901:2701) zeros(1,900)];
POSmusic = imregionalmax(Pmusic);              %MATLAB rtn that finds
local maxima->BW array "1"s
PEAKmusic = find(POSmusic);                    % index pointers to
local Maxima
[bs,is]=sort(Pmusic(find(POSmusic)),'descend'); % sort by highest peak-
>lowest
ThESTmusic= PEAKmusic(is);                     % index to peaks
ThESTmusic= 180*phi(ThESTmusic)/pi ;           % Angle where peaks
occur
thESTmusic=ThESTmusic(1,1:3);
thESTmusic=thESTmusic*pi/180;
```

THIS PAGE INTENTIONALLY LEFT BLANK

LIST OF REFERENCES

[1] F. H. P Fitzek and M. D. Katz, *Cooperation in wireless networks: principles and applications: real egoistic behavior is to cooperate*. Dordrecht, The Netherlands: Springer, 2006.

[2] J. C. Chen and K. Yao, R. E. Hudson, "Source localization and beamforming." *IEEE Signal Processing Magazine*, Mar 2002, vol. 19, pp 30-39.

[3] J. Agre and L. Clare, "An integrated architecture for cooperative sensing networks." *IEEE Computer*, May 2000, vol. 33, pp 106-108

[4] H. Krim and M. Viberg, "Two decades of array signal processing research." *IEEE Signal Processing Magazine*, July 1996, vol. 13, pp 67-94.

[5] R. A. Poisel, *Electronic warfare target location methods*. Norwood, MA: Artech House, 2005.

[6] R. O. Schmidt, "A new approach to geometry of range difference location." *IEEE Trans. on Aerospace and Electronics Systems*, Nov 1972, vol. 8, pp. 821-835.

[7] W. H. Foy, "Position-location solutions by Taylor-series estimation." *IEEE Trans. on Aerospace and Electronics Systems*, March 1976, vol. 12, pp. 187-194.

[8] J. O. Smith and J. S. Abel, "Closed form least squares source location estimation from range difference measurements*." IEEE Trans. on Acoustics, Speech, and Signal Processing*, Dec 1987, vol. 35.

[9] Y. T. Chan and K. C. Ho, "*A* simple and efficient estimator for hyperbolic location*." IEEE Trans. on Signal Processing*, August 1994, vol. 42, pp. 1905-1915.

[10] G. Mellen II, M. Patcher and J. Raquet, "Closed form solution for determining emitter using time difference of arrival measurements." *IEEE Trans. on Aerospace and Electronics Systems*, July 2003, vol. 39, pp. 1056-1058.

[11] A. Lazano, et.al., "Guest editorial-Advances in smart antennas." *IEEE Wireless Communications*, Aug 2006, vol. 13, pp. 6-7.

[12] R. O. Schmidt, "*A signal subspace approach to multiple emitter location and spectral estimation*." Ph.D. Dissertation, Stanford University, 1981.

[13] A. Barrabell, "Improving the resolution performance of eigen-stracture-based-direction finding algorithms." *IEEE Trans. on Acoustics, Speech, and Signal Processing,* Apr 1983, vol.8, pp. 336-339.

[14] R. K. Kumarejan and D. W. Tufts, "Estimating the angles of arrival of multiple plane waves." *IEEE Trans. on Aerospace and Electronics Systems,* January 1983, vol. 19, pp. 134-139.

[15] J. Capon, "High resolution frequency wavenumbers spectrum analysis." *IEEE Proceedings,* August 1969, vol.57.

[16] R. Roy and T. Kaliath, "ESPRIT-estimation of signal parameters via rotational invariant techniques." *IEEE Trans. on Acoustics, Speech, and Signal Processing,* July 1989, vol.37.

[17] J. C. Libert and T. S. Rappaport, *Smart antennas for wireless communications: IS-95 and third generation CDMA applications.* Upper Saddle River, NJ: Prentice Hall, 1999.

[18] A. P. Zamora, J. Vidal and D. H Brooks, "Closed-form solution for positioning based on angle of arrival measurements" *The 13th IEEE International Symposium on Personal, Indoor and Mobile Radio Communications,* September 2002, vol. 4, pp. 1522-1526.

[19] K. R. Deergha and D. C. Reddy, "A new method for finding electromagnetic emmiter location." *IEEE Trans. on Aerospace and Electronics Systems,* October1994, vol. 30, pp. 1081-1085.

[20] K. Spingarn, "Passive position location estimation using the extended Kalman filter." *IEEE Trans. on Aerospace and Electronics Systems,* Jul 1987, vol. 23, pp. 558-567.

[21] H. L. Bertoni, *Radio propagation for modern wireless systems,* Upper Saddle River, NJ: Prentice Hall, 2000.

[22] C. Chen, "A non-line-of–sight error mitigation algorithm in location estimation." *IEEE Wireless Communications and Networking Conference*, September 1999, vol. 1, pp 316-320.

[23] L. Xiong, "A selective model to suppress NLOS signals in angle-of-arrival (AOA) location estimation." Ninth *IEEE International Symposium on Personal, Indoor and Mobile Radio Communications,* September 1998, vol. 1, pp 461-465.

[24] J. L. Conan and S. Pierre, "Using antenna array in multipath environment for wireless sensor positioning." *IEEE Vehicular Technology Conference*, September 2006, vol. 1, pp 1-4.

[25] C. Elam, " *Method and apparatus for space division multiple access receiver,"* Patent No.6,823,021, Rights assigned to in Greenwich Technology Associates, One Soundview Way, Danen, CT. November 23, 2004.

[26] C. Balanis, *Introduction to smart antennas,* Morgan and Claypool Publisher, 2007.

[27] L. C. Godara and A. Cantoni, "Uniqueness and linear independence of steering vector in array space." *The Journal of the Acoustical Society of America,* August 1981, vol. 70, pp. 467-475.

[28] C. W. Therrien, *Discrete random signals and statistical signal processing,* Prentice Hall, 1992.

[29] B. D. Steinberg, *Principles of aperture and array system including random and adaptive arrays,* John Wiley & Sons, New York, 1977.

[30] R. Ertel et al., "Overview of spatial channel models for antenna array communications systems." *IEEE Trans. on Personal Communications,* February 1998, vol. 5, pp 10-22.

[31] T. S Rappaport, *Wireless communications: principles and practice,* Upper Saddle River, NJ: Prentice Hall, 2002.

[32] F. Gross, *Smart antennas for wireless communications,* New York, NY: Mc Graw Hill, 2005.

[33] W. Stallings, *Wireless communications and networks,* Prentice Hall, 2004.

[34] M. O Al-Nuami and M. S Ding, "Prediction models and measurements of microwave signal scattered from building." *IEEE Transactions,* vol. 42, August 1994.

[35] K. I Pedersen, P. E. Mogensen and B. H Fleury, "Power azimuth spectrum in outdoor environments" *IEEE Electronic letters,* vol. 33, August 1997.

[36] I. Pedersen, P. E. Mogensen and B. H Fleury, Spatial channel characteristics in outdoor environments and their impact in B.S antennas system performance." *48th IEEE Vehicular Technology Conference*, May 1998, vol. 2, pp. 713-723.

[37] C. E. Taylor, *Terrestrial communication between wireless sensor networks using beam-forming and space division multiple access,* Master's thesis in Electrical Engineering, Naval Postgraduate School, Monterey, CA, June 2008.

[38] L. C. Godara, "Applications of antenna arrays to mobile communications Part II: beam-forming and direction-of-arrival considerations." *IEEE Proceedings,* August 1997 vol. 85, pp. 1995-1245.

[39] J. Foutz, A. Spanias and M. K. Banavar, *Narrowband direction of arrival estimation for antenna arrays,* Morgan and Claypool Publisher, 2008.

[40] P. F. Driessen, "Measured propagation characteristics of 900 MHz mobile radio channels in mountainous terrain." *40th IEEE Vehicular Technology Conference,* May 1990, vol. 2, pp. 603-609.

[41] H. T. Wu, J. F. Yang and F. K. Chen, "Source number estimators using transformed Gerschgorin radii." *IEEE Trans. on Signal Processing,* June 1995, vol. 43, pp. 1325-1333.

[42] F. Athley, "Optimization of element positions for direction finding with sparse arrays." *11th IEEE Signal Processing Workshop,* 2001, pp. 516-519.

[43] S. O Mantis, *Localization of wireless communication emitters using Time Difference of Arrival (TDOA) methods in noisy channels,* M.S in Electrical Engineering and M.S in Systems Engineering Thesis, Naval Postgraduate School, Monterey, CA, June 2001.

[44] R. M. Brown, "Emitter location using bearing measurements from a moving platform." *Naval Research Laboratory,* Washington D.C, June 1981.

[45] N. Levanon, "Interferometry against differential Doppler: Performance comparison." *IEEE Proceedings on Radar and Signal Processing,* April 1989, vol. 136, pp. 70-74.

[46] G. H. Golumb and C. F. Van Loan, *Matrix computations,* The Johns Hopkins University Press, Baltimore, 1996.

[47] L. N. Trefethen and D. Bau III, *Numerical linear algebra*, SIAM, Philadelphia, 1997.

[48] S. M. Kay, *Fundamentals of statistical processing, volume I: Estimation theory,* Upper Saddle River, NJ: Prentice Hall, 1993.

[49] G. H. Golumb and C. F. Van Loan, "An analysis of the total least squares problem." *SIAM Journal in Numerical Analysis,* 1980, vol. 17, pp. 883-893.

INITIAL DISTRIBUTION LIST

1. Defense Technical Information Center
   Ft. Belvoir, Virginia

2. Dudley Knox Library
   Naval Postgraduate School
   Monterey, California

3. CDR Michael Riggins
   U.S. Special Operations Command
   Tampa, Florida

4. Thomas Kirkpatrick
   Naval Space and Warfare Command – Space Systems Center, Charleston,
   Charleston, South Carolina

5. Michael Niermann
   Naval Space and Warfare Command – Space Systems Center, Charleston,
   Charleston, South Carolina

6. Hellenic Navy General Staff (HNGS)
   Athens, Greece

7. Murali Tummala
   Naval Postgraduate School
   Monterey, California

8. John McEachen
   Naval Postgraduate School
   Monterey, California

9. Owens Walker
   Naval Postgraduate School
   Monterey, California

10. Georgios Tsivgoulis
    Naval Postgraduate School
    Monterey, California